

1 **RNA-directed DNA methylation prevents rapid and heritable reversal of**
2 **transposon silencing under heat stress in *Zea mays*.**

3

4 Wei Guo¹ Dafang Wang² and Damon Lisch^{1*}

5

6 ¹ Department of Botany and Plant Pathology, Purdue University, West Lafayette, Indiana, USA

7 ² Division of Math and Sciences, Delta State University, Cleveland, MS, USA

8 * Corresponding author

9 E-mail: dlich@purdue.edu

10

11 Short title: Rapid and heritable reversal of silencing of a maize transposon.

12

13 **Abstract**

14 In large complex plant genomes, RNA-directed DNA methylation (RdDM) ensures that
15 epigenetic silencing is maintained at the boundary between genes and flanking transposable
16 elements. In maize, RdDM is dependent on *Modifier of Paramutation 1 (Mop1)*, a putative RNA
17 dependent RNA polymerase. Here we show that although RdDM is essential for the maintenance
18 of DNA methylation of a silenced *MuDR* transposon in maize, a loss of that methylation does not
19 result in a restoration of activity. Instead, heritable maintenance of silencing is maintained by
20 histone modifications. At one terminal inverted repeat (TIR) of this element, heritable silencing
21 is mediated via H3K9 and H3K27 dimethylation, even in the absence of DNA methylation. At
22 the second TIR, heritable silencing is mediated by H3K27 trimethylation, a mark normally
23 associated with somatically inherited gene silencing. We find that a brief exposure of high
24 temperature in a *mop1* mutant rapidly reverses both of these modifications in conjunction with a
25 loss of transcriptional silencing. These reversals are heritable, even in *mop1* wild type progeny in
26 which methylation is restored at both TIRs. These observations suggest that DNA methylation is
27 neither necessary to maintain silencing, nor is it sufficient to initiate silencing once has been
28 reversed. However, given that heritable reactivation only occurs in a *mop1* mutant background,
29 these observations suggest that DNA methylation is required to buffer the effects of
30 environmental stress on transposable elements.

31

32 **Author Summary**

33 Most plant genomes are mostly transposable elements (TEs), most of which are held in check by
34 modifications of both DNA and histones. The bulk of silenced TEs are associated with
35 methylated DNA and histone H3 lysine 9 demethylation (H3K9me2). In contrast, epigenetically
36 silenced genes are often associated with histone lysine 27 trimethylation (H3K27me3). Although
37 stress can affect each of these modifications, plants are generally competent to rapidly reset them
38 following that stress. Here we demonstrate that although DNA methylation is not required to
39 maintain silencing of the *MuDR* element, it is essential for preventing heat-induced, stable and
40 heritable changes in both H3K9me2 and H3K27me3 at this element, and for concomitant
41 changes in transcriptional activity. These finding suggest that RdDM acts to buffer the effects of
42 heat on silenced transposable elements, and that a loss of DNA methylation under conditions of
43 stress can have profound and long lasting effects on epigenetic silencing in maize.

44 **Introduction**

45

46 Transposable elements (TEs) are a ubiquitous feature of all genomes. They survive in
47 large measure because they can out-replicated the rest of the genome [1]. As a consequence of
48 that replication, TE can threaten the integrity of the host genome. In response to this threat, all
49 forms of life have evolved mechanisms by which TEs can be silenced when they are recognized
50 as such and, importantly, maintained in a silenced state over long periods of time, even when the
51 initial trigger for silencing is no longer present [2-4]. Because plant genomes are largely
52 composed of TEs, the majority of plant DNA is maintained in an epigenetically silent state [5].
53 Because they are the primary target of epigenetic silencing in plants, TEs are an excellent model
54 for understanding the means by which particular DNA sequences are targeted for silencing, and
55 for understanding the means by which silencing can be maintained from one generation to the
56 next [6]. Finally, because TEs have proved to be exquisitely sensitive to a variety of stresses [7-
57 9], they can also teach us a great deal about the relationship between stress and epigenetically
58 encoded memory of stress.

59 In plants, heritable epigenetic silencing of TEs is almost invariably associated with DNA
60 methylation [10-12]. The vast bulk of TEs in plant genomes are methylated and, with some
61 notable exceptions [13], epigenetically silenced [14, 15]. DNA methylation has a number of
62 features that makes it an appealing mechanism by which silencing can be heritably propagated,
63 either following cell divisions during somatic development, or transgenerationally, from one
64 generation to the next. Because methylation in both the CG and CHG sequence contexts (where
65 H = A, T or G) are symmetrical, information concerning prior DNA methylation can be easily
66 propagated by methylating newly synthesized DNA strands using the parent strand as a template.
67 For CG methylation, this is achieved by reading the methylated cytosine using VARIANT IN
68 METHYLATION 1-3 (VIM1-3) [16, 17] and writing new DNA methylation using the methyl
69 transferase MET1 [18-20]. For CHG, methylation is read indirectly by recognition of H3K9
70 dimethylation (H3K9me2) by CMT3, which catalyzes methylation of newly synthesized DNA,
71 which in turn triggers methylation of H3K9 [21-23].

72 Maintenance methylation of most CHH involves RNA-directed DNA methylation
73 (RdDM). The primary signal for *de novo* methylation of newly synthesized DNA from
74 previously methylated DNA sequences is thought to be transcription by DNA POLYMERASE

75 IV (POLIV) of short transcripts from previously methylated templates [24-26]. This results in the
76 production of small RNAs that are tethered to the target DNA by DNA POLYMERASE IV
77 (POLV), which is targeted by SU(VAR)3-9 homologs SUVH2 and SUVH9, which bind to
78 methylated DNA [27]. This in turn triggers *de novo* methylation of newly synthesized DNA
79 strands using the methyl transferases DRMT1/2 [28, 29]. In addition to the RdDM pathway,
80 CHH methylation can also be maintained due to the activity of CHROMOMETHYLASE
81 (CMT2), which, similar to CMT3, works in conjunction with H3K9me2 to methylate non-CG
82 cytosines, particularly in deeply heterochromatic regions of the genome [30]. Finally, because
83 both histones and DNA must be accessible in order to be modified, chromatin remodelers such as
84 DDM1 are also often required for successful maintenance of TE silencing [23, 31]. In plants,
85 effective silencing of TEs requires coordination between DNA methylation and histone
86 modifications [32]. Together, these pathways can in large part explain heritable propagation of
87 both DNA methylation and histone modification of TEs.

88 In large genomes such as that of maize, much of RdDM activity is focused not on deeply
89 silenced heterochromatin, which is often concentrated in pericentromeric regions, but on regions
90 immediately adjacent to genes, referred to as “CHH islands” because genes in maize are often
91 immediately adjacent to silenced TEs [15, 33]. In maize, mutations in components of the RdDM
92 pathway affect both paramutation and transposon silencing. Mutations in *Modifier of*
93 *Paramutation 1 (Mop1)*, a homolog of *RNA DEPENDENT RNA POLYMERASE2 (RDR2)*, result
94 in the loss of nearly all 24 nucleotide small RNAs, as well as the CHH methylation that is
95 associated with them [34-36]. Despite this, *mop1* has only minimal effects gene expression in
96 any tissue except the meristem [33, 37], and the plants are largely phenotypically normal. This,
97 along with similar observations in Arabidopsis, has led to the suggestion that the primary role of
98 RdDM is to reinforce boundaries between genes and adjacent TEs, rather than to regulate gene
99 expression [33].

100 Unlike animals, plants do not experience a global wave of DNA demethylation either in
101 the germinal cells of the gametophyte or the in early embryo [38]. Thus, DNA methylation and
102 associated histone modifications are an attractive mechanism for transgenerationally propagated
103 silencing. Indeed, there is strong evidence that mutants that trigger a global loss of methylation
104 can cause heritable reactivation of previously silenced TEs, although it is worth noting that even
105 in mutants in which the vast majority of DNA methylation has been lost, only a subset of TEs are

106 transcriptionally reactivated [39, 40], and DNA methylation of many TEs can be rapidly
107 reestablished at many loci via RdDM in wild type progenies of mutant plants, suggesting that
108 memory propagated via DNA methylation can be restored due to the presence of small RNAs
109 that can in trigger *de novo* methylation of previously methylated sequences [41, 42].

110 In contrast to TEs, most genes that are silenced during somatic development in plants are
111 associated with H3K27 trimethylation (H3K27me3), which requires the activity of the polycomb
112 complexes PRC2 and PRC1, which together catalyze H3K27 methylation and facilitate its
113 heritable propagation [43-45]. In plants, H3K27me3 enrichment is generally associated with
114 genes rather than TEs [46, 47]. The most well explored example of this involves epigenetic
115 setting of FLC, a negative regulator of flowering in Arabidopsis [48, 49]. In a process known as
116 vernalization, prolonged exposure to cold results in somatically heritable silencing of this gene,
117 which in turn results in flowering under favorable conditions in the spring. Somatically heritable
118 silencing of FLC is initially triggered by non-coding RNAs, which are involved in recruitment of
119 components of PRC2, which catalyze H3K27 trimethylation, which in turn mediates a
120 somatically heritable silent state [48]. Importantly, H3K27 trimethylation at genes like FLC is
121 erased each generation, both in pollen and in the early embryo [50-52]. The fact that H3K27me3
122 must be actively reset suggests that in the absence of this resetting, H3K27me3 in plants is
123 competent to mediate transgenerational silencing but is normally prevented from doing so.

124 Dramatic differences in TE content between even closely related plant species suggest
125 that despite the relative stability of TE silencing under laboratory conditions, TEs frequently
126 escape silencing and proliferate in natural settings [53]. Stress, both biotic and abiotic can often
127 trigger TE transcription and, at least in some cases, transposition [7, 54-57]. Further, there is
128 evidence that the association of TEs and genes can result in *de novo* stress induction of adjacent
129 genes [54, 58, 59].

130 Because of its dramatic and global effects on both gene expression and protein stability,
131 heat stress has attracted considerable attention, particularly with respect to heritable transmission
132 of TE activity. For both genes and TEs, although heat stress can trigger somatically heritable
133 changes in gene expression, there appear to be a variety of mechanisms to prevent or gradually
134 ameliorate transgenerational transmission of those changes [60, 61]. Thus, for instance, although
135 the Onsen retrotransposon is sensitive to heat, it is only in mutants in the RdDM pathway that
136 transposed elements are transmitted to the next generation [9, 62]. Given that both TEs and

137 various components of regulatory pathways that have evolved to regulated them are up-regulated
138 in germinal lineages, this is not surprising [63, 64]. Similar experiments using silenced
139 transgenes have demonstrated that double mutants of *mom1* and *ddm1* cause these transgenes as
140 well as several TEs to be highly responsive to heat stress, and the observed reversal of silencing
141 can be passed on to a subsequent generation, but only in mutant progeny [65]. It is also worth
142 noting that in many cases of TE reactivation, silencing is rapidly re-established in wild type
143 progeny [66, 67]. The degree to which this is the case likely depends on a variety of factors, from
144 the copy number of a given element, its position within the genome, its mode of transposition
145 and the presence or absence of trans-acting small RNAs targeting that TE [68].

146 Our model for epigenetic silencing is the *Mutator* system of transposons in maize. The
147 *Mutator* system is a family of related elements that share similar, 200 bp terminal inverted
148 repeats but that contain distinct internal sequences. Nonautonomous *Mu* elements can only
149 transpose in the presence of the autonomous element, *MuDR*. *MuDR* is a member of the MULE
150 superfamily of Class II cut and paste transposons [69, 70]. In addition to being required for
151 transposition, the 200 bp TIRs within *MuDR* elements serve as promoters for the two genes
152 encoded by *MuDR*, *mudrA*, which encodes a transposase, and *mudrB*, which encodes a novel
153 protein that is required for *Mu* element integration. Both genes are expressed at high levels in
154 rapidly dividing cells, and expression of both of them is required for full activity of the *Mutator*
155 system [71, 72]. MURA, the protein produced by *mudrA*, is sufficient for somatic excision of *Mu*
156 elements, which results in characteristically small revertant sectors in somatic tissue. *MuDR*
157 elements can be heritably silenced when they are in the presence of *Mu killer (Muk)*, a
158 rearranged variant of *MuDR* whose transcript forms a hairpin that is processed into 21-22 nt
159 small RNAs that directly trigger transcriptional gene silencing (TGS) of *mudrA* and indirectly
160 trigger silencing of *mudrB* when it is in trans to *mudrA* [4, 73]. Because *Muk* can be used to
161 heritably silence *MuDR* through a simple cross, and because silencing of *MuDR* can be stably
162 maintained after *Muk* is segregated away, the *MuDR/Muk* system is an excellent model for
163 understanding both initiation and maintenance of silencing. Prior to exposure to *Muk*, *MuDR* is
164 fully active and is not prone to spontaneous silencing [74]. After exposure, *MuDR* silencing is
165 exceptionally stable over multiple generations [73].

166 When *mudrA* is silenced, DNA methylation in all three sequence contexts accumulates
167 within the 5' end of the TIR immediately adjacent to *mudrA* (TIRA) [75]. Methylation at the 5'

168 and 3' portions of this TIR have distinctive causes and consequences. The 5' end of the TIR is
169 readily methylated in the absence of the transposase, but this methylation does not induce
170 transcriptional silencing of *mudrA* [76]. Methylation in this end of TIRA is readily eliminated in
171 the presence of functional transposase. However, the loss of methylation in a silenced element in
172 this part of the TIRA does not result in heritable reactivation of a silenced element. In contrast,
173 CG and CHG methylation the 3' portion of TIRA, which corresponds to the *mudrA* transcript as
174 well as to *Muk*-derived 22 nt small RNAs that trigger silencing, is not eliminated in the presence
175 of active transposase and is specifically associated with heritable transcriptional silencing of
176 *mudrA*.

177 The second gene encoded by *MuDR* elements, *mudrB*, is also silenced by *Muk*, but the
178 trajectory of silencing of this gene is entirely distinct, despite the fact that the *Muk* hairpin has
179 near sequence identity to the TIR adjacent to *mudrB* (TIRB) [4, 73]. By the immature ear stage
180 of growth in F1 plants that carry both *MuDR* and *Muk*, *mudrA* is transcriptionally silenced and
181 densely methylated. In contrast, *mudrB* in intact elements remains transcriptionally active in this
182 tissue, but its transcript is not polyadenylated. It is only in the next generation that steady state
183 levels of transcript become undetectable. Further, experiments using deletion derivatives of
184 *MuDR* that carry only *mudrB* are not silenced by *Muk* when they are on their own, or when they
185 are in trans to an intact *MuDR* element that is being silenced by *Muk*. This suggests that heritable
186 silencing of *mudrB* is triggered by the small RNAs that target *mudrA*, but the means by which
187 this occurs is indirect and involves spreading of silencing information from *mudrA* to *mudrB*.

188 Silencing of *mudrA* can be destabilized by the *mop1* mutant, a homolog of RNA-
189 DEPENDENT RNA POLYMERASE2 (RDR2) that is required for the production of the vast
190 bulk of 24 nt small RNAs in maize, including those targeting *Mu* TIRs [34-36, 77]. However
191 silencing of *MuDR* by *Muk* is unimpeded in a *mop1* mutant background, likely because *Muk*-
192 derived small RNAs are not dependent on *mop1* [78]. Further, although reversal of silencing of
193 *MuDR* in a *mop1* mutant background does occur, it only occurs gradually, over multiple
194 generations, and only affects *mudrA*. In contrast, *mudrB* is not reactivated in this mutant
195 background and, because *mudrB* is required for insertional activity, although these reactivated
196 elements can excise during somatic development, they cannot insert into new positions.

197
198

199 **Results**

200

201 **DNA methylation is not required to maintain silencing of *MuDR* elements in *mop1* mutants.**

202 Given that *MuDR* elements are only activated after multiple generations in a *mop1*
203 mutant background, we wanted to understand how silencing of *MuDR* is maintained in *mop1*
204 mutants prior to reactivation. To do this, we examined expression and DNA methylation at TIRA
205 by performing bisulfite sequencing of TIRA of individuals in families that were segregating for a
206 single silenced *MuDR* element, designated *MuDR**, and that were homozygous or heterozygous
207 for *mop1* (Fig 1A and Fig S1).

208 In control plants carrying an active *MuDR* element, all cytosines in TIRA were
209 unmethylated, which was consistent with our previous results and which indicated that bisulfite
210 conversion was efficient (Fig 1B). Also consistent with previous results, F₂ *MuDR*^{*/-}; *mop1*^{/+}
211 plants, whose F₁ parent carried both *MuDR* and *Muk*, exhibited dense methylation at TIRA. In
212 contrast, DNA methylation in the CG, CHH and CHG contexts at TIRA was absent in *mop1*
213 mutant siblings. Interestingly, *mop1* had effects on TIRB that are more consistent with the
214 known effects of this mutant specifically on CHH methylation. While F₂ *MuDR*^{*/-}; *mop1*^{/+}
215 plants exhibited dense methylation at TIRB in all sequence contexts, *mop1* homozygous siblings
216 exhibited a loss of methylation only in the CHH context. Despite the effects of *mop1* on *MuDR*
217 methylation at both TIRA and TIRB, RT-PCR results demonstrated that these *mop1* mutant
218 plants did not exhibit reactivation of *mudrA* or *mudrB* (Fig 1C).

219

220 ***MOP1* enhances enrichment of H3K9 and H3K27 dimethylation at TIRA.**

221 Transposon silencing is often associated with H3K9 and H3K27 dimethylation, two
222 hallmarks of transcriptional silencing in plants [21, 47]. DNA methylation, particularly in the
223 CHG context, is linked with H3K9 dimethylation through a self-reinforcing loop, and these two
224 epigenetic marks often colocalize at TEs and associated nearby genes [79]. We had previously
225 demonstrated that these two repressive histone modifications corresponded well with DNA
226 methylation of silenced *MuDR* elements at TIRA [75]. However, our observation that silencing
227 of *mudrA* can be maintained in the absence of DNA methylation in *mop1* mutants suggests that
228 additional repressive histone modifications may be responsible for maintaining the silenced state
229 of *mudrA*. To test this hypothesis, we examined the enrichment of H3K9me₂ at TIRA in

230 individuals in a family that segregated for silenced *MuDR* and for *mop1* homozygotes and
231 heterozygotes (Fig 1A) by performing a chromatin immunoprecipitation quantitative PCR (ChIP-
232 qPCR) assay. As controls, we also examined these two histone modifications in leaf tissue from
233 plants carrying active and deeply silenced *MuDR* elements in a wild type background. Compared
234 with active *MuDR*^{-/-}; +/+ plants, H3K9me2 and levels were significantly enriched at TIRA in the
235 *MuDR*^{*/-}; +/+ plants (Fig 2A). The same was true of H3K27me2 (Fig S2). Surprisingly, a
236 significant increase in H3K9me2 and H3K27me2 at TIRA was observed in *mop1* mutants
237 compared with their sibling *mop1* heterozygous siblings and with the silenced *MuDR*^{*/-}; +/+
238 control plants, suggesting that the loss of DNA methylation that resulted from the loss of MOP1
239 in these mutants actually resulted in an increase in both of these repressive chromatin marks.

240

241 **Silencing of TIRB is associated with an increase in H3K27me3.**

242 Like *mudrA*, *mudrB* is silenced by *Muk*, but maintenance of *mudrB* silencing has distinct
243 requirements. Unlike *mudrA*, which is eventually reactivated in a *mop1* mutant background
244 under normal conditions, *mudrB* remains silenced, suggesting that maintenance of silencing of
245 this gene is independent of *MOP1* [35]. ChIP-qPCR revealed that silencing of *mudrB* is not
246 associated with H3K9me2 methylation. Instead, heritably silenced TIRB is enriched for
247 H3K27me3, a modification normally associated with somatically silenced genes rather than
248 transposable elements (Fig 2B). The *mop1* mutant appears to enhance H3K27me3 at TIRB
249 relative to the *mop1* heterozygous siblings, although the enrichment is no greater than observed in
250 the *MuDR*^{*/-}; +/+ controls.

251

252 **Application of heat stress specifically in the early stage of growth can promote the** 253 **reactivation of silenced *MuDR* elements in *mop1* mutants**

254 There is ample evidence that a variety of stresses can reactivate epigenetically silenced
255 TEs. One particularly effective treatment is heat stress. Given that a loss of methylation by itself
256 is not sufficient to reactivate silenced *MuDR* elements, we subjected *mop1* mutant and *mop1*
257 heterozygous sibling seedlings carrying silenced *MuDR* elements (*MuDR*^{*}) to heat stress.
258 Fourteen-day-old *MuDR*^{*/-}; *mop1/mop1* and *MuDR*^{*/-}; *mop1/+* sibling seedlings were heated at
259 42 °C for four hours and leaf samples were collected immediately after that treatment (Fig 3A).

260 RT-PCR for the heat response factor Hsp90 (Zm00001d024903) confirmed that the seedlings
261 were responding to the heat treatment (Fig S3). We then examined *MuDR* transcription by
262 performing RT-PCR on RNA from leaf three immediately after the plants had been removed
263 from heat and from control plants that had not been subjected to heat stress. In the *mop1* mutants,
264 both *mudrA* and *mudrB* became transcriptionally reactivated upon heat treatment (Fig 3B).
265 *MuDR* elements in plants that were *mop1* mutant that were not heat stressed and were those that
266 were wild type and that were heat stressed were not reactivated, demonstrating that both a mutant
267 background and heat stress are required for efficient reactivation. To determine if the application
268 of heat stress at a later stage of plant development can also promote reactivation, we heat-
269 stressed 28-day-old plants and examined *MuDR* transcription in leaf seven at a similar stage of
270 development (~10 cm) as had been examined in heat stressed leaf three in the previous
271 experiment. In these plants, we saw no evidence of reactivation, indicating that *MuDR*
272 responsiveness to heat shifts over developmental time (Fig 3C). Taken together, these data
273 suggest that the application of heat stress specifically at an early stage of plant development can
274 promote the reactivation of a silenced TE in a mutant that is deficient in the RdDM pathway.

275 TIRA in a *mop1* mutant background already lacks any DNA methylation prior to heat
276 treatment and thus heat would not be expected to reduce TIRA methylation. However in *mop1*
277 mutants TIRB retained CG and CHG methylation and also remained inactive (Fig 1B). To
278 determine if reactivation after heat treatment is associated with a loss of this methylation, we
279 examined DNA methylation at TIRB in *mop1* mutants in the presence or absence of heat
280 treatment. This assay was performed on the same tissues that we collected for *MuDR* expression
281 reactivation analysis. We found that the DNA methylation pattern was the same for both the heat
282 treated and the control *mop1* mutant plants, indicating that heat stress does not alter TIRB
283 methylation and that a further loss of DNA methylation is not the cause of *mudrB* reactivation in
284 this tissue (Fig S4).

285 **Heat stress reverses TE silencing by affecting histone modifications at TIRA and TIRB**

286 Under normal conditions, we found that H3K9me2 at TIRA is associated with silencing,
287 and H3K9me2 is actually enriched when TIRA methylation is lost in *mop1* mutants (Fig 2A). In
288 contrast, we find that H3K27me3, rather than H3K9me2, is enriched at TIRB and is maintained
289 at similar or slightly elevated levels in *mop1* mutant relative to *mop1* heterozygous siblings (Fig

290 2B). Given these observations, we hypothesized that heat stress may reverse H3K9me2
291 enrichment at TIRA and H3K27me3 enrichment at TIRB. To test this hypothesis, we determined
292 the level of H3K9me2 and H3K27me3 at TIRA and TIRB under normal and stressed conditions
293 using ChIP-qPCR.

294 Upon heat stress, the level of H3K9me2 at TIRA was significantly decreased in *mop1*
295 mutants compared to that of non-treated *mop1/mop1* mutant siblings (Fig 4A). Interestingly,
296 however, H3K9me2 enrichment only decreased to the level observed at TIRA in silenced
297 *MuDR*^{*-/}; +/+ plants, and it remained significantly higher than that of TIRA in the naturally
298 active *MuDR*^{-/}; +/+ plants. In contrast, we observed no changes in H3K27me3 at TIRA.

299 At TIRB, we observed no changes in H3K9me2 enrichment in any of our samples.
300 Instead, we found that heat treatment reversed previously established H3K27me3 at TIRB,
301 supporting the hypothesis that this modification, rather than H3K9me2, mediates heritable
302 silencing of *mudrB* (Fig 4B). Consistent with evidence for transcriptional activation of both
303 *mudrA* and *mudrB*, we observed enrichment of the active mark H3K4me3 in reactivated TIRA
304 and TIRB (Fig 4C,D). Taken together, these data demonstrate that heat stress can simultaneously
305 reduce two often mutually exclusive repressive histone modifications, H3K9me2 and
306 H3K27me3 at the two ends of a single TE.

307

308 **The reactivation state is somatically transmitted to the new emerging tissues**

309 We next sought to determine whether or not the reactivated state can be propagated to
310 cells in somatic tissues after the heat had been removed. We performed quantitative RT-PCR to
311 detect *mudrA* and *mudrB* transcripts in mature leaf ten of plants 35 days after the heat stress and
312 in immature tassels ten days after that. At V2, when the heat stress was applied and leaf three
313 was assayed, cells within leaf 10 primordia are present and may have experienced the heat stress.
314 In contrast, because the tassel primordia are not formed until V5, the cells of the tassel could not
315 have experienced the heat stress directly [80, 81]. We found that both genes stayed active in both
316 tissues, indicating heat-induced reactivation is stably transmitted to new emerging cells and
317 tissues (Fig 5).

318

319 ***MuDR* activity is stably heritably transmitted to subsequent generations**

320 Our previous work had demonstrated that silenced *mudrA* (but not *mudrB*) can be progressively

321 and heritably reactivated only after multiple generations of exposure to the *mop1* mutation under
322 normal conditions. Only after eight generations could this activity could be stably transmitted to
323 subsequent generations in the absence of the *mop1* mutation [35]. To determine if the somatic
324 activity we observed after heat stress can be transmitted to the next generation, we crossed the
325 heat-treated *mop1* homozygous plants that carried transcriptionally reactivated *MuDR*
326 (designated *MuDR*[~]) and the sibling *mop1* homozygous *MuDR*^{*} control plants, to a tester that
327 was homozygous wild type for *mop1* and that lacked *MuDR* (Fig S1). MURA, the protein
328 encoded by *mudrA* causes excision of a reporter element at the *a1-mum2* allele of the *Al* gene,
329 resulting pale kernels with spots of colored revertant tissue. All plants used in these experiments
330 were homozygous for *a1-mum2*. If *mudrA* were fully heritably reactivated, a cross between a
331 *MuDR*^{-/-}; *mop1/mop1* plant and a tester would be expected to give rise to 50% spotted kernels,
332 and this phenotype would be expected to cosegregate with the reactivated *MuDR* element. The
333 progeny of ten independent heat-reactivated individuals gave a total of 45% spotted kernels. In
334 contrast, ten *mop1* homozygous siblings that carried *MuDR*^{*} and that had not been heat treated
335 gave rise to an average of only 0.7% spotted kernels after test crossing (Fig 6B, Supplemental
336 Table 1). These results show that *MuDR* activity induced by heat treatment was transmitted to
337 the next generation. RT-PCR in both endosperms and embryos of the spotted and pale progeny
338 kernels and genotyping for the presence or absence of *MuDR* at position 1 on chromosome 9L
339 [74] demonstrated that activity was transmitted to both the embryo and the endosperm, and that
340 this activity cosegregated with the single *MuDR* present in these families (Fig S3). We employed
341 a similar strategy to test stability of heritability. We crossed three subsequent generations to
342 testers and counted the spotted kernels. We observed that the progeny of heat-reactivated
343 individuals gave a total of 51%, 48% and 47% spotted kernels in the three subsequent
344 generations. In contrast, subsequent generations of the lineage carrying *MuDR*^{*} that had not been
345 heat treated gave rise to only a small number of weakly spotted kernels (Fig 6C, D, Supplemental
346 Table 1). These results demonstrate that heat reactivation is stable over multiple generations in a
347 non-mutant genetic background, as is silencing in the absence of heat stress.

348

349 **DNA hypomethylation is not associated with transgenerational inheritance of activity**

350 We have shown that DNA methylation is not reduced under heat stress at TIRB, and that
351 even a complete absence of methylation of TIRA under normal conditions does not result in

352 transcriptional activation. These results suggest that, at least under normal conditions, DNA
353 methylation of *MuDR* is neither necessary nor sufficient to mediate silencing. However, only
354 plants that were *mop1* mutant and whose TIRs were missing either methylation of cytosines in
355 all sequence contexts in the case of TIRA or those in the CHH sequence context in the case of
356 TIRB were reactivated under heat stress. This suggests that a loss of methylation may be a
357 precondition for initiation, and perhaps propagation, of continued activity after that stress. To test
358 the later possibility, we examined DNA methylation at TIRA and TIRB in the *mop1*
359 heterozygous H₂ progenies of heat-reactivated *mop1* mutant plants and those of their unheated
360 *mop1* mutant sibling controls (Fig S1). Surprisingly, we found that both TIRA and TIRB were
361 extensively methylated in all three sequence contexts in all progeny examined regardless of their
362 activity status (Fig 7). Indeed, their methylation was indistinguishable from that observed at
363 silenced *MuDR* elements. This suggests that after reactivation, although the restoration of MOP1
364 does result in the restoration of methylation at both TIRA and TIRB, this methylation is not
365 sufficient for reestablishment of silencing at either of these TIRs. In order to determine whether
366 DNA methylation we observed in these wild type H₂ plants was stable, we examined TIRA and
367 TIRB methylation in plants four generation removed from the initial heat stress. Surprisingly, we
368 found that the observed patterns of methylation in this generation at both TIRs closely resembled
369 that of fully active *MuDR* elements (Fig 7). This suggests that patterns of methylation consistent
370 with activity are in fact restored in the heat stressed lineage, but only after multiple rounds of
371 meiosis in a non-mutant genetic background.

372

373 **Transgenerational heritability of activity is associated with heritability of histone** 374 **modifications**

375 DNA hypomethylation is not associated with transgenerational inheritance of *MuDR*
376 activity, and DNA hypermethylation does not result in a restoration of silencing in wild type
377 progeny of heat reactivated mutants. A plausible alternative is that the observed changes in
378 histone marks mediate heritable propagation of activity of both *mudrA* and *mudrB* independent
379 of methylation status. To test this hypothesis, we determined the levels of H3K9me₂, H3K27me₃
380 and H3K4me₃ at TIRA and TIRB in the *mop1* heterozygous H₂ progenies of heat-reactivated
381 *MuDR*^{-/-}; *mop1/mop1* plants and those of their sibling untreated *MuDR*^{*/-}; *mop1/mop1* sibling
382 controls. Consistent with the continued activity of *mudrB* in the progeny of the heat stressed

383 plants, relative levels of H3K27me3 levels remained low and H3K4me3 remained high at TIRB
384 in these plants, suggesting that heritable propagation of H3K27me3 is responsible for that
385 continued activity (Fig 8). Similarly, at TIRA, H3K9me2 remained low and H3K4me3 remained
386 high in these progenies. Interestingly, the increase in DNA methylation in these *MuDR* active
387 *mop1* heterozygous plants was associated with a further decrease in levels of H3K9me2 at TIRA
388 relative to that of their heat stressed *mop1* homozygous parents, down to the levels of the active
389 *MuDR* control. This suggests that a increase in methylation of these active elements in the wild
390 type background resulted in a concomitant decrease in H3K9me2 at TIRA.

391

392 **Discussion**

393

394 **DNA methylation is neither necessary nor sufficient for the maintenance of silencing at** 395 **TIRA or TIRB**

396 Our results demonstrating that methylation is not necessary for maintenance of epigenetic
397 silencing in *mop1* mutant plants (Fig 1) and is not sufficient to trigger silencing in H2 reactivated
398 plants (Fig 7) suggest that at this particular locus, DNA methylation is not the key determinative
399 factor with respect to either silencing or its reversal. In contrast, changes in H3K9me2 are
400 closely correlated with changes in TIRA activity, suggesting that it is this modification, rather
401 than DNA methylation, that mediates both activity and heritable transmission of silencing of
402 *mudrA*. Given that H3K9me2 is normally tightly associated with cytosine methylation,
403 particularly in the CHG context [21, 82], this result is unexpected. However, our results clearly
404 demonstrate that this modification can be heritably propagated in the absence of DNA
405 methylation and in the absence of the original trigger for silencing, *Muk*. Even more unexpected
406 is our observation that, once *mudrA* becomes silenced, in *mop1* mutants there appears to be
407 reciprocal relationship between DNA methylation of TIRA and H3K9me2 enrichment. Based on
408 previous experiments, our expectation was that *mop1* would eliminate cytosine methylation in
409 the 5' end of TIRA, which is unrelated to transcriptional gene silencing of *mudrA*, but that it
410 would not elimination of DNA methylation in the 3' portion of TIRA, which is primarily in the
411 CG and CHG contexts and is specifically associated with silencing of this gene [76]. In fact, we
412 find that methylation in all three sequence context is eliminated throughout TIRA in *mop1*
413 mutants, but this does not result in reactivation of *mudrA*. Instead, H3K9me2 actually

414 significantly *increases* in the *mop1* mutant. This suggests that silencing at this locus is
415 maintained via a balance between DNA and histone methylation, such that a loss of DNA
416 methylation actually triggers an increase in histone modification. This in turn suggests that the
417 state of activity of *mudrA* in some way determines the balance between histone and DNA
418 modification, since neither modification by itself appears to be determinative. Our heat
419 experiment supports this hypothesis. Heat rapidly reduces histone modification, but only back
420 down to the level of the silent *mop1* heterozygous siblings rather than to the level of TIRA in an
421 active element. In this case, the combination of an absence of DNA methylation with this
422 reduced level of H3K9me2 appears to be sufficient to permit transcription of *mudrA*, as well as
423 somatic propagation of the reactivated state to daughter cells after the heat is removed. Also
424 supporting a balance hypothesis is the observation that in reactivated *mop1* heterozygous
425 progeny of *mop1* homozygous heat treated plants, methylation is restored to that observed in
426 silenced elements and levels of H3K9 dimethylation are then reduced to the level observed in
427 active elements. This suggests that, again, levels of DNA and histone modification balance each
428 other, such that an increase in methylation in the wild type progeny of reactivated *mop1* mutant
429 plants results in a concomitant decrease in histone modification. Interestingly, however, after
430 multiple generations in a wild type background, methylation levels are reduced to those of active
431 *MuDR* elements, suggesting that this reduced methylation level is a consequence, rather than a
432 cause, of maintenance of activity. Collectively, these data suggest that DNA methylation can be
433 a lagging indicator that is responding to a given epigenetic state, rather than determining it.

434 There are other instances in which silencing can be reversed without a loss of
435 methylation. For instance, mutations in the putative chromatin remodeler MOTHER OF
436 MORPHEOUS1(MOM1) can result in activation of silenced transgenes and some endogenous
437 loci in the absence of a loss of DNA methylation [83-85]. Similarly, Microorchidia (MORC)
438 ATPase genes, as well the H3K27 monomethyltransferases ATXR5 and ATXR6 in Arabidopsis,
439 are required for heterochromatin condensation and TE silencing but not for DNA methylation or
440 histone modification associated with that silencing [86-88]. However, unlike reactivated *MuDR*
441 elements in our experiments, reintroduction of the wild type MOM1 or MORC alleles result in
442 immediate re-silencing. Finally, mutations in two closely related Arabidopsis genes, MAIL1 and
443 MAIN, can also result in activation of a subset of Arabidopsis TEs in the absence of a loss of
444 methylation [89].

445 **The RdDM pathway buffers the effects of heat stress on silenced *MuDR* elements.**

446 Heat stress rapidly reverses silencing and is associated with a reduction of H3K9me2, but only in
447 a *mop1* mutant background. This suggests that although DNA methylation is not required for the
448 maintenance of silencing of *mudrA* and is not sufficient to trigger *de novo* silencing of this gene,
449 it is required to prevent a response to heat stress. Thus, we suggest that the primary role of DNA
450 methylation in this instance is to buffer the effects of heat. We note that this observation is
451 similar but distinct from what has been observed for the Onsen retrotransposon in Arabidopsis.
452 In that case, although heat stress by itself can induce transcription of Onsen [9, 90], it is only
453 when the RdDM pathway is deficient that new insertions are transmitted to the next generation.
454 However in wild type progenies of heat stressed mutants, Onsen elements are rapidly re-silenced
455 [91]. In contrast, reactivated *MuDR* elements remain active for at least five generations, despite
456 the fact that the RdDM pathway rapidly restores DNA methylation at both TIRA and TIRB. This
457 is likely due to differences between these two elements with respect to the means by which the
458 two elements are maintained in a silenced state. In the absence of *Muk*, *MuDR* elements are
459 stably active over multiple generations [74, 92]. This suggests that silencing of *MuDR* requires
460 aberrant transcripts that are distinct from those produced by *MuDR* that are not present in the
461 minimal Mutator line. Experiments involving some low copy number elements in Arabidopsis
462 that are activated in the DNA methylation deficient *ddm1* mutant background suggest that the
463 same is true for these elements as well; once activated, these elements remain active even in wild
464 type progeny plants [93]. In contrast, evidence from other TEs suggests that transcripts from
465 these elements or their derivatives contribute to their own silencing [39, 94, 95].

466

467 **Heritably transmitted silencing of TIRB is associated with H3K27me3**

468 Our observation that transgenerationally heritable silencing of *mudrB* is associated with
469 H3K27me3 was surprising, given that this mark is generally associated with somatic silencing of
470 genes that is reset each generation [96]. However, in the absence of that resetting, silencing can
471 be heritably transmitted to the next generation [50, 52]. Our data clearly shows that this is the
472 case for *mudrB*, whose H3K27me3 enrichment can be heritably transmitted following the loss of
473 *Mu killer* through at least two rounds of meiosis, and we have evidence that *mudrB* remains
474 stably silenced for at least eight generations [35]. Given that there is no selective pressure to
475 reset TE silencing mediated by H3K27me3, this is not surprising.

476 There is evidence that heat stress can heritably reverse H3K27me3 at specific loci.
477 H3K27 trimethylation can be reversed by the H3K27me3 demethylase REF6, which acts in
478 conjunction the chromatin remodeler BRAHMA (BRM) to relax silencing at loci containing
479 CTCTGYTY motifs [97]. In Arabidopsis, under heat stress, HEAT SHOCK TRANSCRIPTION
480 FACTOR A2 (HSFA2) activates REF6, which can in turn de-repress HSFA2 by reducing
481 H3K27me3 at this gene. This feedback loop can extend to the progeny of heat stressed plants,
482 resulting in a heritable reduction in levels of H3K27me3 at REF6 target genes [98, 99].
483 However, as in the case for all transgenerational shifts in gene expression, the effect is
484 temporary, and both H3K27me3 and gene expression levels are restored to their original state
485 after two generations.

486

487 **Conclusions**

488 There is a growing body of evidence suggesting that whatever else they do, all silencing
489 pathways can and do silence TEs, and in many cases may have evolved to do so. For instance
490 H3K27me3 is largely associated with gene rather than TE silencing in higher plants, the
491 bryophyte *Marchantia polymorpha*, which diverged from extant land plants 400 mya, appears to
492 employ H3K27me3 as a mark for a substantial fraction of its heterochromatin, in place of
493 H3K9me2 [100]. Similarly, a majority of silenced maternal copies of paternally expressed genes
494 in Arabidopsis are marked by H3K27me3 in addition to H3K9me2 and DNA methylation [101].
495 There is also evidence that the original, ancestral role of H3K27me3 may be in TE regulation. In
496 the single celled ciliate, *Paramecium tetraurelia*, loss of function of the Enhancer-of-zeste-like
497 protein Ezl1, which can catalyze methylation of both H3K9 and H3K27, results in global de-
498 repression of TEs with minimal effects on gene expression [102]. In multicellular organisms,
499 epigenetic silencing of cell lineages via this pathway simplifies the problem of differentiation by
500 heritably silencing whole suites of genes in tissues in which they are not needed. Single celled
501 organisms do not have that requirement, but, like all other organisms, they do have a requirement
502 to heritably silence TEs.

503 Overall, our data suggests that even when examining a single TE in a single organism, a
504 wide variety of epigenetic processes can be seen to play a role in both silencing and its reversal.
505 At TIRA, a loss of DNA methylation in *mop1* mutants is associated with what appears to be a
506 compensatory increase in H3K9me2, which is heritably reversed by a brief exposure to heat.

507 Heritable transmission of a reactivated state of *mudrA* is refractive to a restoration of DNA
508 methylation, which instead appears to adjust over time to reflect that activity rather than to block
509 it. In contrast to *mudrA* (and most other TE genes) heritable *mudrB* silencing is associated with
510 H3K37me3 enrichment, which, like H3K9me2 enrichment at TIRA, is readily and heritably
511 reversed by heat treatment. At both TIRA and TIRB, methylation is neither necessary nor
512 sufficient for silencing, but a lack of MOP1 and an associated loss of DNA methylation at both
513 TIRs does appear to be required to precondition both *mudrA* and *mudrB* for responsiveness to
514 heat, consistent with a role for RdDM in buffering the effects of high temperature in maize.
515 Clearly, these results are primarily phenomenological, as the precise mechanism for the reversal
516 of silencing we observe remains a mystery. However, they do suggest that there is a great deal
517 that we do not yet understand about how silenced states can be maintained and how they can
518 be reversed.

519

520 **Materials and Methods**

521

522 **Plant materials**

523 Maize seedlings and adult plants were grown in MetroMix under standard long-day
524 greenhouse conditions at 26°C unless otherwise noted. The minimal Mutator line consists of one
525 full-length functional *MuDR* element and one nonautonomous *Mutator* element, *Mu1*. *Mu killer*
526 (*Muk*), a derivative version of the *MuDR* transposon, can heritably trigger epigenetic silencing of
527 that transposon. *Mutator* activity is monitored in seeds via excisions of a *Mu1* element inserted
528 into the *a1-mum2* allele of the *A1* gene, resulting in small sectors of revertant tissue, or spots, in
529 the kernels when activity is present. When *MuDR* activity is absent, the kernels are pale. All
530 plants described in these experiments are homozygous for *a1-mum2*. Although *MuDR* can be
531 present in multiple copies, all of the experiments described here have a single copy of *MuDR* at
532 position 1 on chromosome 2L [92].

533 All of the crosses used to generate the materials examined in this paper are depicted in
534 Fig S1. Active *MuDR*⁻;*mop1*/*mop1* plants were crossed to *Muk*⁻;*mop1*/*mop1*⁺ plants. The resulting
535 progeny plants were genotyped to screen for plants that carried *MuDR*, *Muk* and that were
536 homozygous for *mop1*, which were designated F₁ plants. F₁ plants were then crossed to *mop1*
537 heterozygotes. Progeny plants lacking *Muk* but carrying silenced *MuDR* elements, designated

538 *MuDR**, were designated F₂ *MuDR** progeny. F₂ *MuDR** progeny that were homozygous for
539 *mop1* were crossed to *mop1* heterozygotes. The resulting F₃ plants were genotyped for the
540 presence of *MuDR*. These plants were either homozygous or heterozygous for in *mop1*. These F₃
541 plants were those that were used for the heat stress experiments. H1 refers to the first generation
542 of these F₃ plants that were subjected to heat stress, with successive generations designated H₂,
543 H₃, etc... *MuDR* was genotyped using primers Ex1 and RLIR2. Because Ex1 is complementary
544 to sequences flanking *MuDR* in these families, this primer combination is specific to the single
545 *MuDR* element segregating in these families. *Muk* was genotyped using primers TIRAout and
546 12-4R3. The *mop1* mutation was genotyped using primers ZmRDR2F, ZmRDR2R and TIR6. All
547 primer sequences are provided in Table S2.

548

549 **Tissue Sampling**

550 Plants used in all experiments were genotyped individually. The visible portion of each
551 developing leaf blade, when it was ≈ 10 cm, was harvested when it emerged from the leaf whorl.
552 Only leaf blades of mature leaves were harvested. For the heat reactivation experiment, seedlings
553 were grown at 26 °C for 14 days with a 12-12 light dark cycle. Seedlings were incubated at
554 42 °C for 4 hours and leaf 3 was harvested immediately after stress treatment. As a control, leaf 3
555 was also collected from sibling seedlings grown at 26 °C. For each genotype and treatment, 12
556 biological replicates were used, all of which were siblings. Samples were stored in -80 °C. After
557 sample collection, all seedlings were transferred to a greenhouse at 26 °C. In order to determine
558 if reactivation could be propagated to new emerging tissues, leaf 10 at a similar stage of
559 development (~ 10 cm, as it emerged from the leaf whorl) and the immature tassel (~ 20 cm) were
560 collected from each individual (Fig. 4A). To determine if the application of heat stress at a later
561 stage of plant development can promote reactivation, an independent set of these seedlings from
562 the same family were used. A similar strategy was employed. However, in this case, seedlings
563 were heat stressed for 4 hours after the plants had grown 28 days at 26 °C. Leaf 7 was collected
564 instead (Fig. 3B). For the bisulfite sequencing experiment, leaf 3 was collected from each
565 individual, when it was ≈ 10 cm, as it emerged from the leaf whorl. In order to minimize potential
566 variation among different individuals, leaves from 6 individuals with the same genotype and
567 treatment were pooled together. For the CHIP assays, a total of ~ 2 g of leaves from leaf 3 of 6
568 sibling plants with the indicated genotypes was harvested. Three independent sets of these

569 sample collections were collected and analyzed for each genotype and treatment. Leaf samples
570 were fixed with 1% methanol-free formaldehyde and then stored in -80 °C.

571

572 **RNA isolation and RT-PCR analysis**

573 Total RNA was extracted using TRIzol reagent (Invitrogen) and purified by Zymo
574 Direct-zol™ RNA Miniprep Plus kit. 2 µl of total RNA was first loaded on a 1% agarose gel to
575 check for good quality. Then, RNA was quantified by a NanoDrop™ spectrophotometer
576 (Thermo Fisher Scientific) and reverse transcribed using an oligo-dT primer and GoScript™
577 Reverse Transcriptase (Promega). The resulting transcribed cDNA was amplified for 29 cycles
578 with primers specific for the alanine aminotransferase (*Aat*) transcripts (Zm00001d014258) with
579 an annealing temperature of 55 °C used as a control to ensure equal starting amounts of cDNA.
580 Samples were then amplified for 32 cycles using the primers specific for *mudrA* and *mudrB* with
581 an annealing temperature of 59°C for both primer pairs. PCR products were electrophoresed on a
582 1.2% agarose gel. Quantitative RT-PCR was performed by using SYBR Premix Ex Taq™
583 (TaKaRa Bio) on a ABI StepOnePlus™ Real-Time PCR thermocycler (Thermo Fisher
584 Scientific) according to the manufacturer's instructions. Expression of *ZmHsp90*
585 (Zm00001d024903) shown in Fig S3 was measured using primers HSP90-qPCR_F and HSP90-
586 qPCR_F. Relative expression values for all experiments were calculated based on the expression
587 of the reference gene, *ZmTub2* (Zm00001d050716) using primers TUB2-qPCR_F and TUB2-
588 qPCR_R and determined by using the comparative CT method. Sequences for all primers used
589 for RT-PCR are available in Table S2.

590

591 **Genomic Bisulfite Sequencing**

592 These experiments were performed as previously described [76]. In brief, genomic DNA
593 was isolated and digested with RNase A (Thermo Fisher Scientific). 2 µl of this DNA was
594 loaded on a 1% agarose gel to check for good quality and then quantified using a Qubit
595 fluorometer (Thermo Fisher Scientific). 0.5-1 µg of genomic DNA from each genotype and
596 treatment were used for bisulfite conversion. The EZ DNA Methylation-Gold kit (Zymo
597 Research) was used to perform this conversion. Fragments from TIRA and TIRB were PCR-
598 amplified using EpiMark Hot Start Taq DNA Polymerase (New England BioLabs). For TIRA,
599 the first amplification was for 20 cycles using p1bis2f and TIRAbis2R with an annealing

600 temperature of 48 °C, followed by re-amplification for 17 cycles using TIRAbis2R and
601 TIRAmF6 with an annealing temperature of 50 °C. Amplicons from TIRB were amplified for 30
602 cycles using methy_TIRBF and methy_TIRBR with an annealing temperature of 55 °C. The
603 resulting fragments were purified and cloned into pGEM®-T Easy Vector (Promega). Ligations
604 and transformations were performed as directed by the manufacturer's instructions. The resulting
605 colonies were screened for the presence of insertions by performing a colony-based PCR using
606 primers of pGEMF and pGEMTR with an annealing temperature of 52 °C. The sequences of all
607 primers are provided in Table S1. Plasmid was extracted from positive colonies using the Zippy
608 Plasmid Kit (Zymo Research). Plasmid from at least 10 independent clones were sequenced at
609 Purdue Genomics Core Facility. The sequences were analyzed using kismeth
610 (<http://katahdin.mssm.edu/kismeth/revpage.pl>)[103].

611

612 **Chromatin Immunoprecipitation (ChIP)**

613 The ChIP assay was performed as described previously with some modifications [104-
614 106]. Briefly, leaf samples were treated with 1% methanol-free formaldehyde for 15 minutes
615 under vacuum. Glycine was added to a final concentration of 125 mM, and incubation was
616 continued for 5 additional minutes. Plant tissues were then washed with distilled water and
617 homogenized in liquid nitrogen. Nuclei were isolated and resuspended in 1 mL nuclei lysis
618 buffer (50 mM Tris-HCl pH8, 10 mM EDTA, 0.25% SDS, protease inhibitor). 50 µl of nuclei
619 lysis was harvested for a quality check. DNA was sheared by sonication (Bioruptor™ UCD-200
620 sonicator) sufficiently to produce 300 to 500 bp fragments. After centrifugation, the supernatants
621 were diluted to a volume of 3 mL in dilution buffer (1.1% Triton X-100, 1.2mM EDTA, 16.7mM
622 Tris-HCl pH8, 167mM NaCl). Each sample of supernatant was sufficient to make 6
623 immunoprecipitation (IP) reactions. Every 500 µl sample was precleared with 25 µl protein A/G
624 magnetic beads (Thermo Fisher Scientific) for 1 hour at 4 °C. After the beads were removed
625 using a magnet, the supernatant was removed to a new pre-chilled tube. 50 µl from each sample
626 was used to check for sonication efficiency and set aside to serve as the 10% input control.
627 Antibodies used were anti-H3K9me2 (Millipore), H3K27me2 (Millipore), H3K27me3 (Active
628 Motif), H3K4me3 (Millipore) and H3KAc (Millipore). After incubation overnight with rotation
629 at 4°C, 30 µl of protein A/G magnetic beads was added and incubation continued for 1.5 hours.

630 The beads were then sequentially washed with 0.5 mL of the following: low salt wash buffer (20
631 mM Tris (pH 8), 150 mM NaCl, 0.1% (wt/vol) SDS, 1% (vol/vol) Triton X-100, 2 mM EDTA),
632 high salt wash buffer (20 mM Tris (pH 8), 500 mM NaCl, 0.1% (wt/vol) SDS, 1% (vol/vol)
633 Triton X-100, 2 mM EDTA), LiCl wash buffer (10 mM Tris (pH 8), 250 mM LiCl, 1% (wt/vol)
634 sodium deoxycholate, 1% (vol/vol) NP-40 substitute, 1 mM EDTA), TE wash buffer (10 mM
635 Tris (pH 8), 1 mM EDTA). After the final wash, the beads were collected using a magnet and
636 resuspended with 200 μ l X-ChIP elution buffer (100 mM NaHCO₃, 1% (wt/vol) SDS). A total of
637 20 μ l 5M NaCl was then added to each tube including those samples used for quality checks.
638 Cross-links were reversed by incubation at 65 °C for 6 hours. Residual protein was digested by
639 incubating with 20 μ g protease K (Thermo Fisher Scientific) at 55 °C for 1 hour, followed by
640 phenol/chloroform/isoamyl alcohol extraction and DNA precipitation. Final precipitated DNA
641 was dissolved in 50 μ l TE. Quantitative RT-PCR was performed by using SYBR Premix Ex
642 Taq™ (TaKaRa Bio) on an ABI StepOnePlus™ Real-Time PCR thermocycler (Thermo
643 Fisher Scientific) according to the manufacturer's instructions. The primers used in this study are
644 listed in Table S2. The primers used to detect H3K9 and H3K27 dimethylation of Copia
645 retrotransposons and H3K4 trimethylation of actin that were used as internal controls in this
646 study have been validated previously [106]. Primers used for TIRA (TIRAR and TIRAUTRR)
647 and TIRB (Ex1 and RL TIR2) were those used previously to detect changes in chromatin at these
648 TIRs [75]. Expression values were normalized to the input sample that had been collected earlier
649 using the comparative CT method.

650

651 **Acknowledgements**

652 We thank R. Keith Slotkin for critical reading of the manuscript and Anthony Canon for testing
653 the stability of transgenerational heritability.

654

655

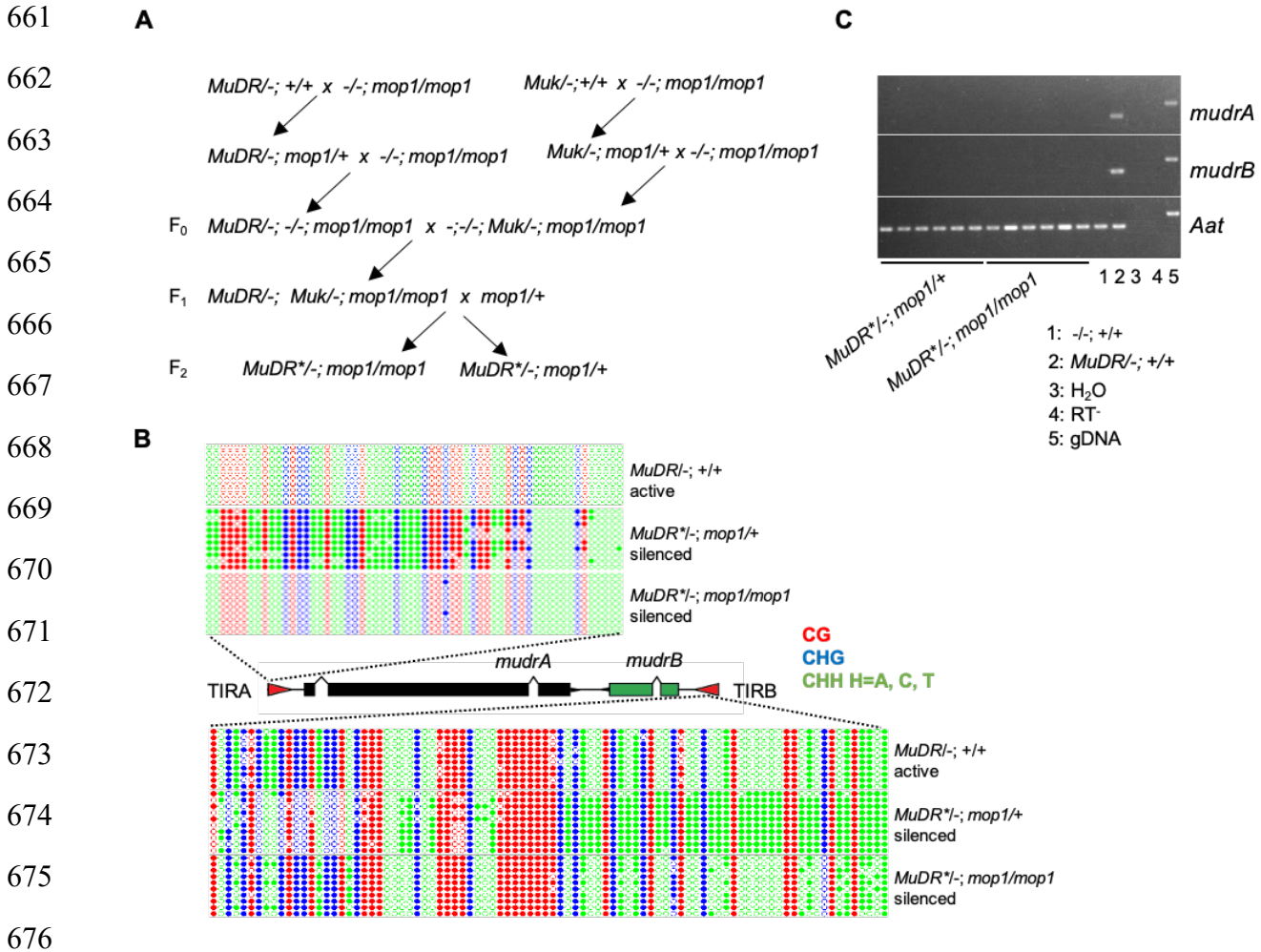
656

657

658

659

660 **Figures**



677 **Figure 1. DNA methylation patterns at TIRA and TIRB of stably silenced F₂ plants.** (A)

678 Crosses used to generate the materials analyzed. (B) DNA methylation patterns at TIRA and

679 TIRB. Ten individual clones were sequenced from amplification of bisulfite-treated samples of

680 the indicated genotypes. The cytosines in different sequence contexts are represented by different

681 colors (red, CG; blue, CHG; green, CHH, where H=A, C, or T). For each genotype, DNA from

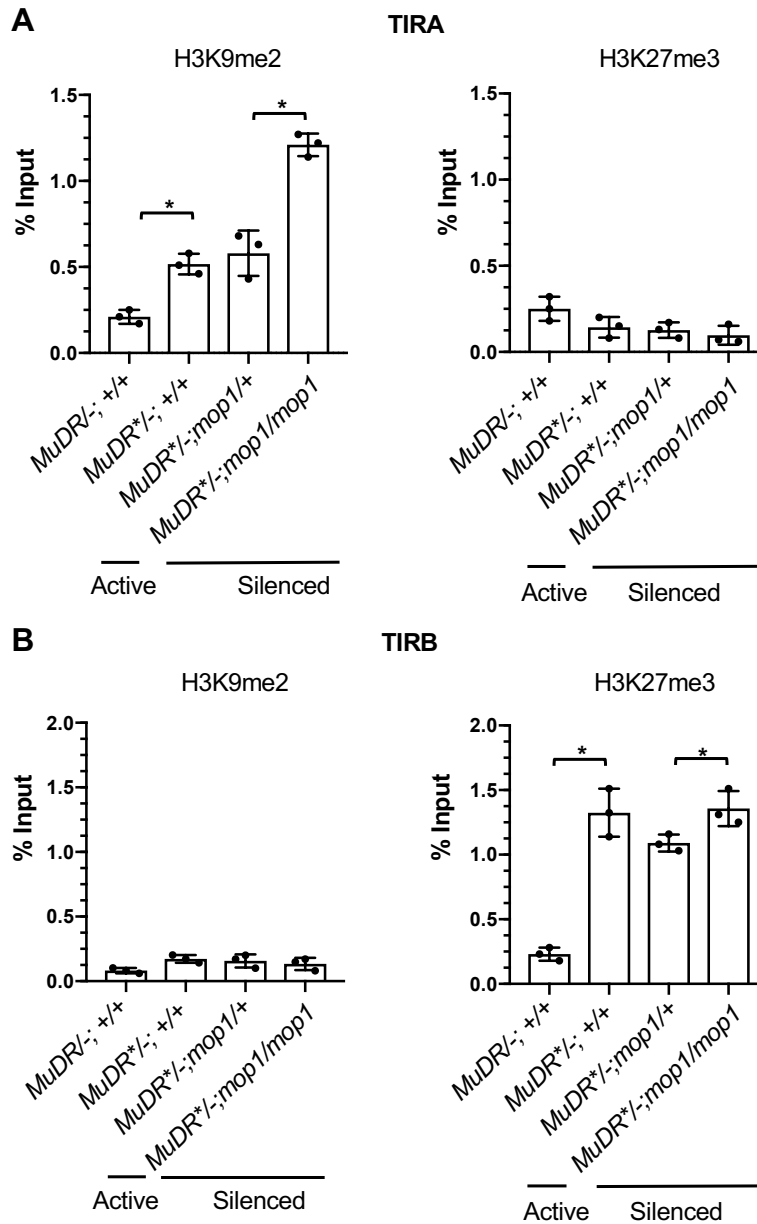
682 six biological replicates were pooled. (C) RT-PCR detecting *mudrA* and *mudrB* transcripts in F₂

683 plants from a family segregating for a single silenced *MuDR* element (*MuDR*^{*}), *mop1/+* and

684 *mop1/mop1*. H₂O: water control. RT⁻: no reverse transcriptase added. gDNA: genomic DNA.

685
686
687

688
689
690
691
692
693
694
695
696
697
698
699
700
701
702
703
704
705
706
707
708
709
710



711 **Figure 2. ChIP-qPCR analysis of enrichment of histone marks H3K9me2 and H3K27me3**
712 **at TIRA and TIRB in *mop1* mutants.** ChIP-qPCR analysis of enrichment of histone marks,
713 H3K9me2 and H3K27me3 at TIRA and TIRB. (A) Relative enrichment of H3K9me2 and
714 H3K27me3 in leaf 3 of plants of the indicated genotypes. *MuDR*: active element. *MuDR**:
715 inactive element. (B) Relative enrichment of H3K9me2 and H3K27me3 in leaf 3 of plants of the
716 indicated genotypes. qPCR signal was normalized to *Copia* and then to the value of input
717 sample. All data are the average of two technical replicates from three independent lines. An

718 unpaired t-test was performed. Error bars indicate mean \pm standard deviation (SD) of the three
 719 biological replicates. *P<0.05; **P < 0.01

720

721

722

723

724

725

726

727

728

729

730

731

732

733

734

735

736

737

738

739

740

741

742

743

744

745

746

747

748

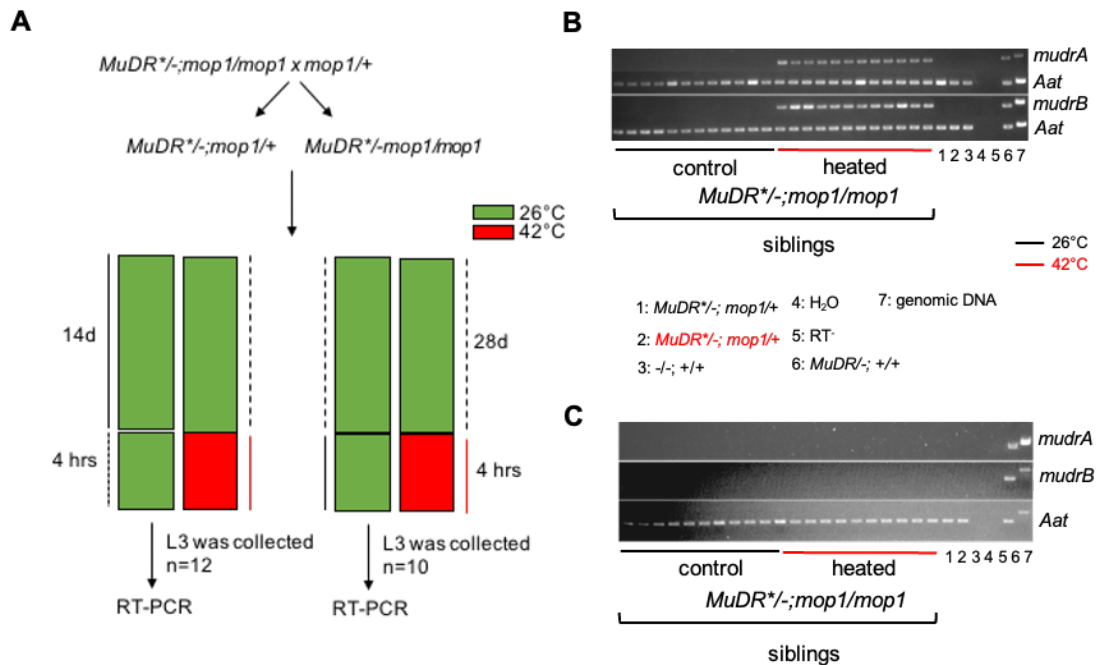


Figure 3. Expression of *mudrA* and *mudrB* in plants under heat stress. (A) Schematic diagram of the heat-reactivation experiment. (B) RT-PCR of *mudrA* and *mudrB* in plants of the indicated genotypes. (C) RT-PCR of *mudrA* and *mudrB* of leaf 7 of heat-treated F2 plants. *Aat* is a housekeeping gene that was used as a positive expression control. Additional controls for each experiment included pools of ten *MuDR^{-/-}; mop1/+* heated and ten unheated plants, as well as plants that lacked *MuDR* and were wild type for *mop1* (*-/-; +/+*), samples with water or with no reverse transcriptase as negative controls, active *MuDR* as well as genomic DNA (gDNA) as positive controls for the *MuDR*-specific PCR primers.

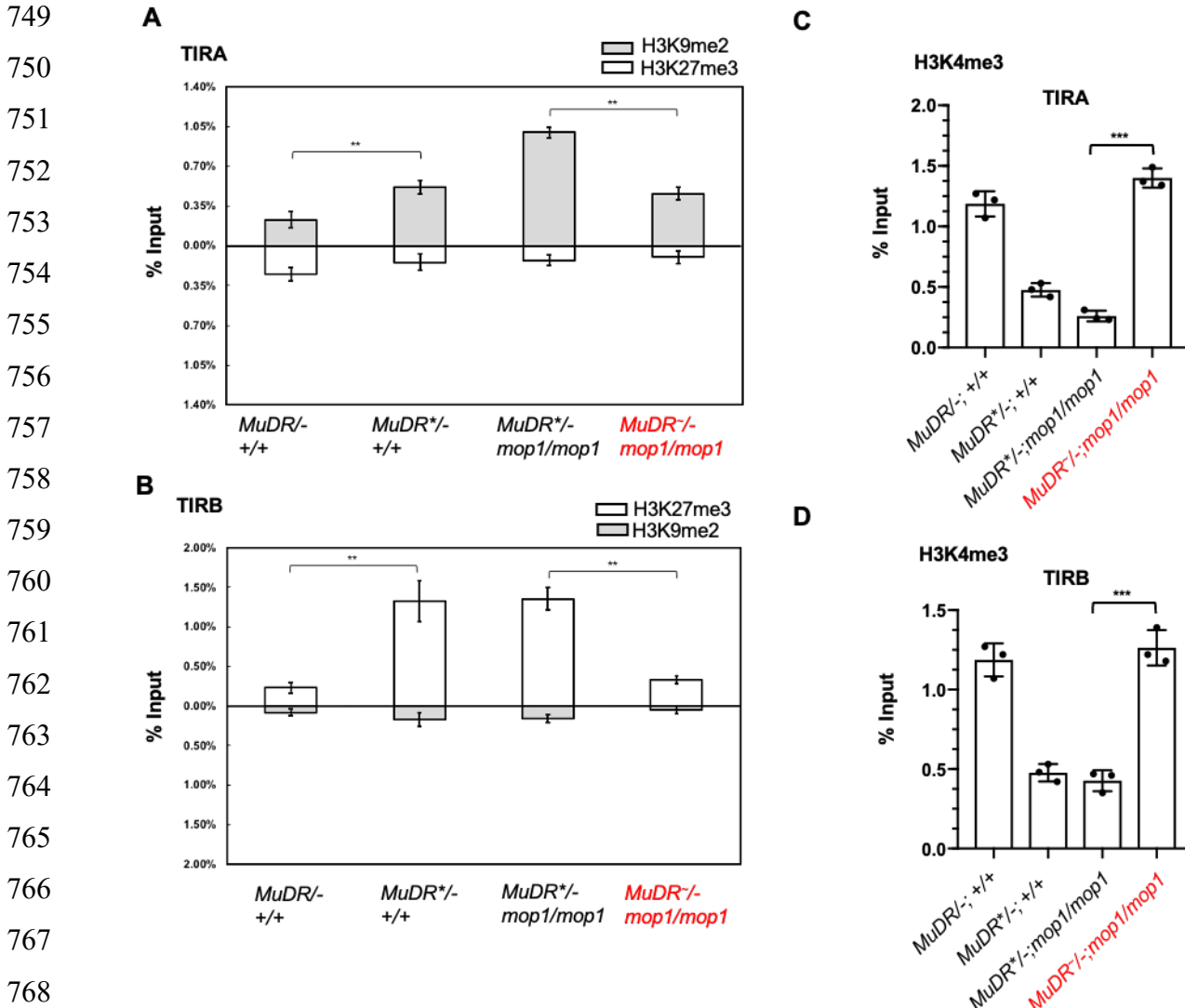


Figure 4. ChIP-qPCR analysis of histone marks TIRA and TIRB under heat stress. Relative enrichment of H3K9me2 and H3K27me3 at TIRA (A) and TIRB (B) in leaf 3 of plants of the indicated genotypes. (Relative enrichment of H3K4me3 at TIRA (C) and TIRB (D) in leaf 3 of plants of the indicated genotypes. qPCR signals were normalized to *Copia* and then to the value of input samples. All data are the average of two technical replicates from three independent lines. An unpaired t-test was performed. Error bars indicate mean \pm standard deviation (SD) of the three biological replicates. **P < 0.01; ***P < 0.001

776
777
778
779

780
781
782
783
784
785
786
787
788
789
790
791
792
793
794
795
796
797
798
799
800
801
802
803
804
805
806
807
808
809

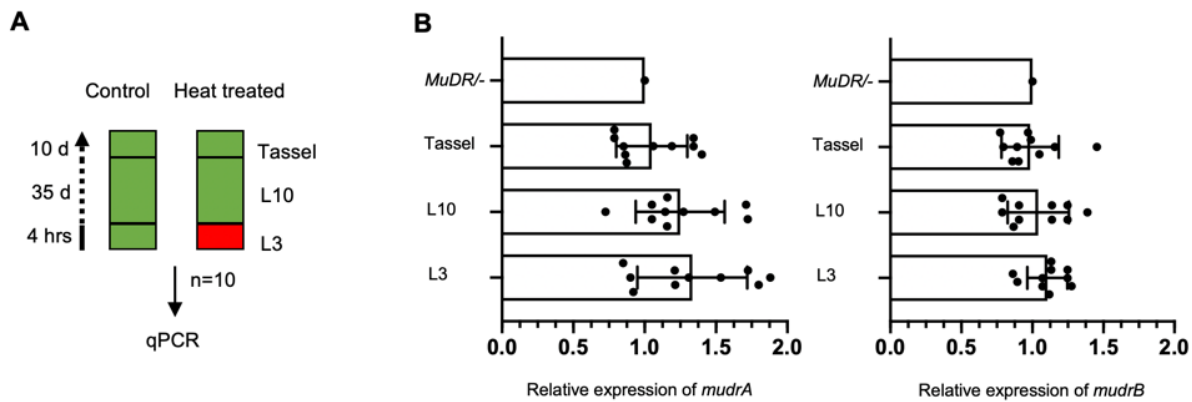
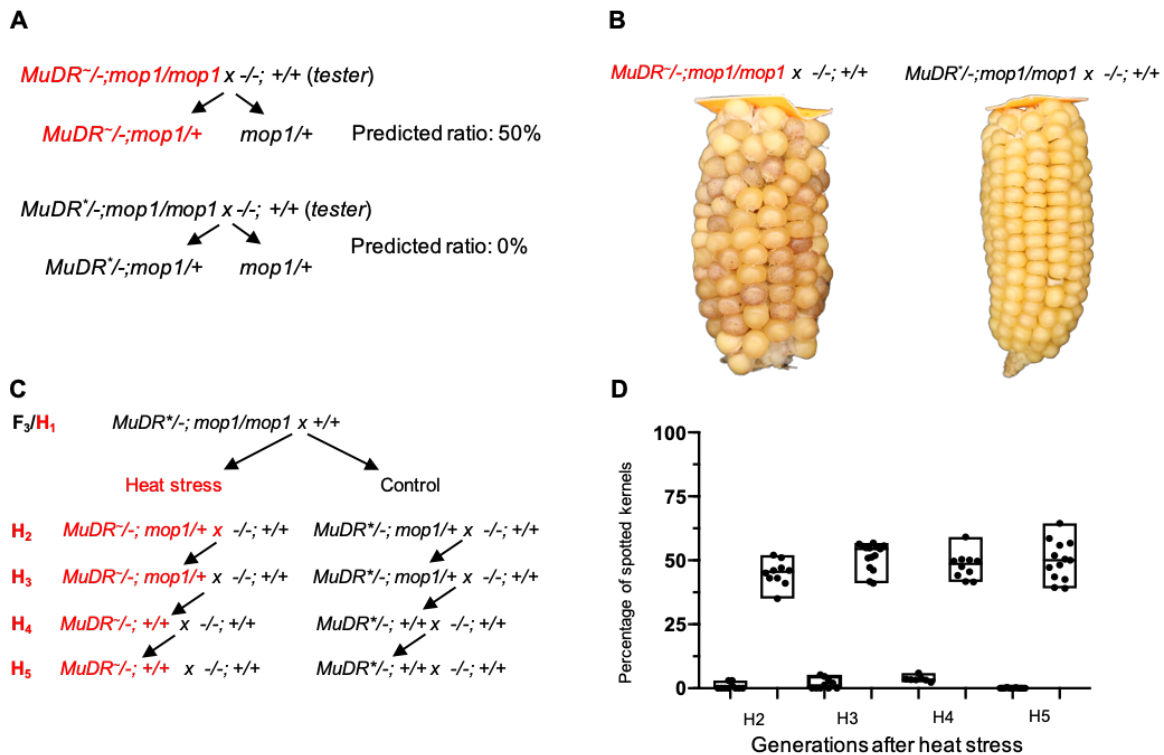
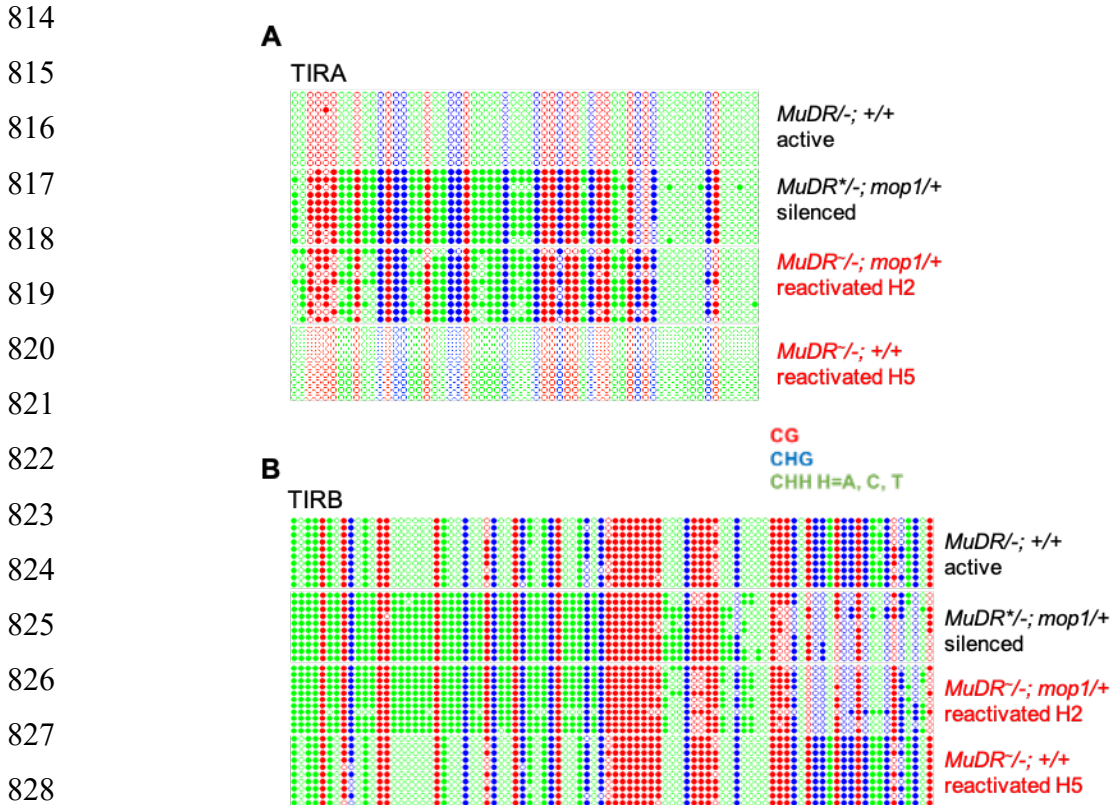


Fig 5. Expression of *mudrA* and *mudrB* in new emerging tissues following heat stress. (A) Diagram of the experiment. (B) qPCR was performed to measure transcript levels of *mudrA* and *mudrB* using expression of maize *Tub2* as an internal control. Expression levels were normalized to that of an active *MuDR* element, which was set at one. All data are the average of two technical replicates from ten independent plants. An unpaired t-test was performed. Error bars indicate mean \pm standard deviation (SD) of the ten biological replicates.



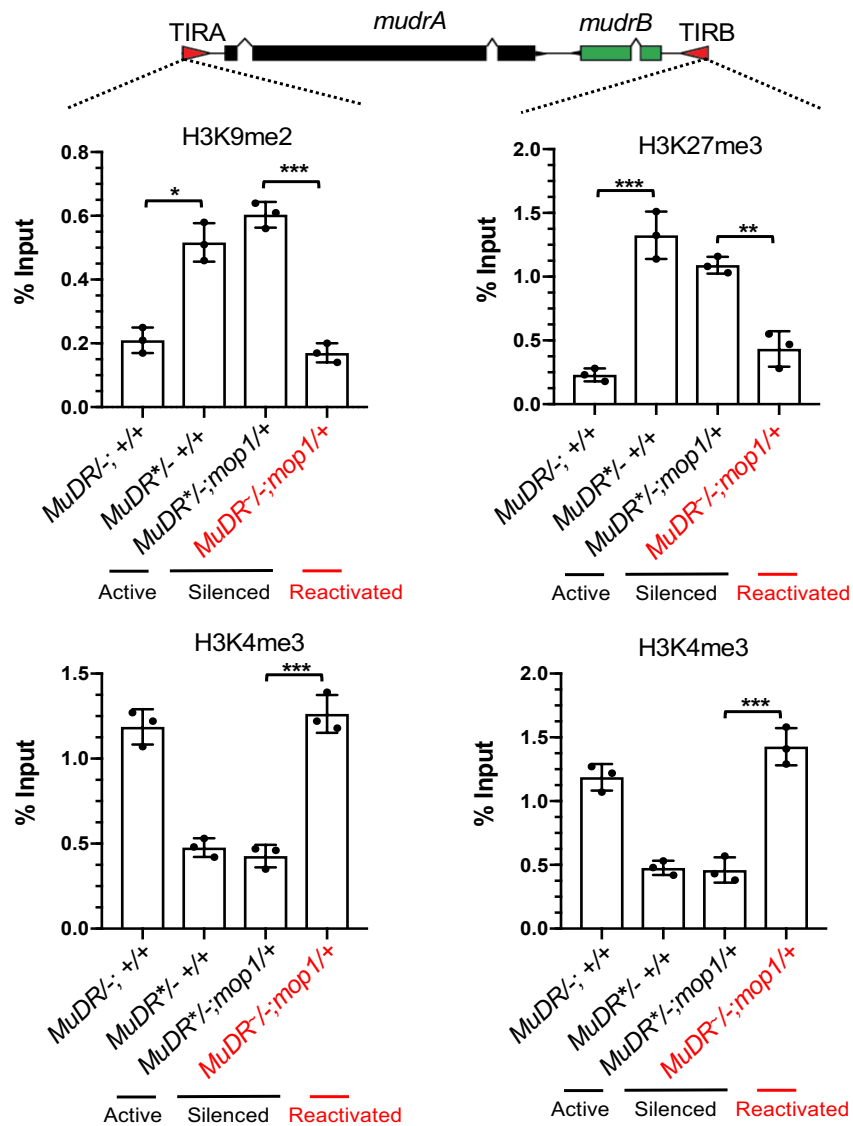
810 **Figure 6. Testing transgenerational inheritance.** (A) A schematic diagram showing the
811 crosses used to determine transgenerational inheritance. (B) Ear ears derived from heat treated
812 and control individuals. (C) Ratios of spotted kernels in generations of wild type plants following
813 the heat stress (H1) generation.



830 **Figure 7. DNA methylation patterns at TIRA and TIRB of progeny of heat-treated H₂ and**
831 **H₅ plants.** (A) DNA methylation patterns at TIRA. (B) DNA methylation patterns at TIRB. Ten
832 individual clones were sequenced from each amplification of bisulfite-treated sample. The
833 cytosines in different sequence contexts are represented by different colors (red, CG; blue, CHG;
834 green, CHH, where H=A, C, or T). For each assay, six independent samples were pooled
835 together.

836
837
838
839
840

841
842
843
844
845
846
847
848
849
850
851
852
853
854
855
856
857
858
859
860
861
862



863 **Figure 8. ChIP-qPCR analysis of enrichment of histone marks, H3K9me2, H3K27me3 and**
864 **H3K4me3 at TIRA and TIRB.** Relative enrichment of H3K9me2, H3K27me3 and H3K4me3
865 at TIRA and TIRB in leaf 3 of plants of the indicated genotypes. qPCR signals were normalized
866 to *Copia* and then to the value of input samples. All data are the average of two technical
867 replicates from three independent lines. An unpaired t-test was performed. Error bars indicate
868 mean \pm standard deviation (SD) of the three biological replicates. *P<0.05; **P < 0.01;
869 ***P<0.001

870
871

872 **Supplemental Figures**

873

874

875

876

877

878

879

880

881

882

883

884

885

886

887

888

889

890

891

892

893

894

895

896

897

898

899

900

901

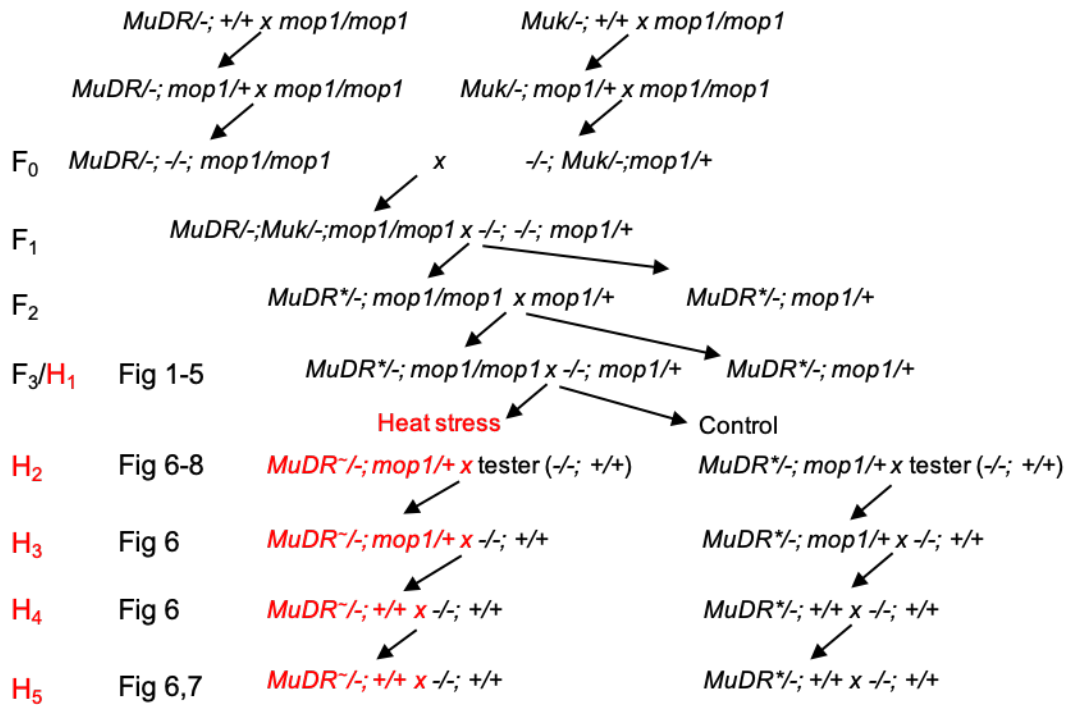


Fig S1. Diagram of the crosses and generations used in this study. F1 refers to the first generation during which *MuDR* was exposed to *Muk*. H₁, which corresponds to F₃, is the generation in which a brief heat treatment was applied. *MuDR* indicates an active *MuDR* element. *MuDR** indicates an inactive *MuDR* element. *MuDR~* indicates a reactivated *MuDR* element.

902
903
904
905
906
907
908
909
910
911
912
913
914
915
916
917
918
919
920
921
922
923
924
925
926
927
928
929
930
931
932

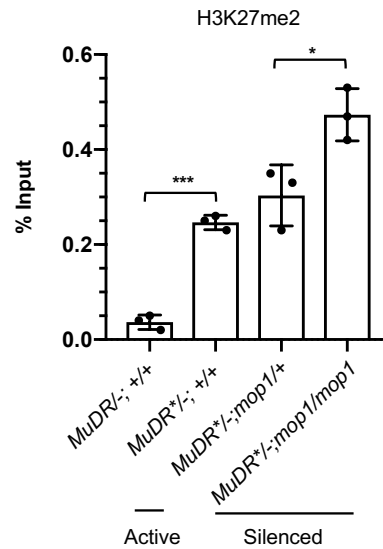


Fig S2. ChIP-qPCR analysis of enrichment of H3K27me2 at TIRA. Relative enrichment of H3K27me2 at TIRA in leaf 3 of plants of the 4 indicated genotypes. The qPCR values were normalized to *Copia* and then to the value of input samples. All data are the average of two technical replicates from three independent sibling plants. An unpaired t-test was performed. Error bars indicate mean \pm standard deviation (SD) of the three biological replicates. * $P < 0.05$; *** $P < 0.001$

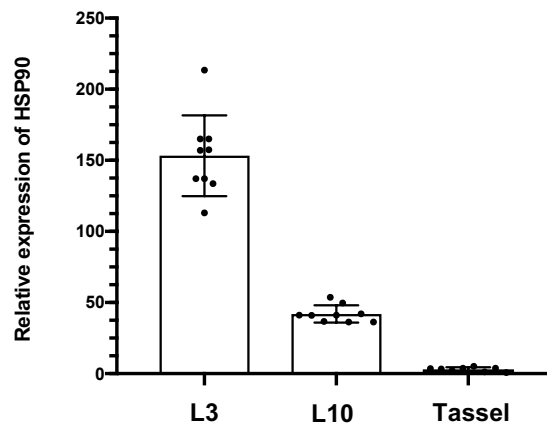
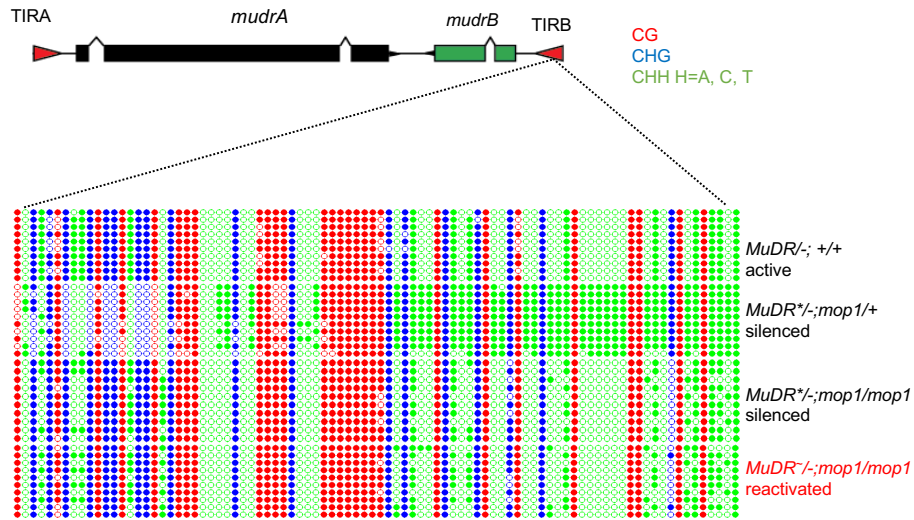


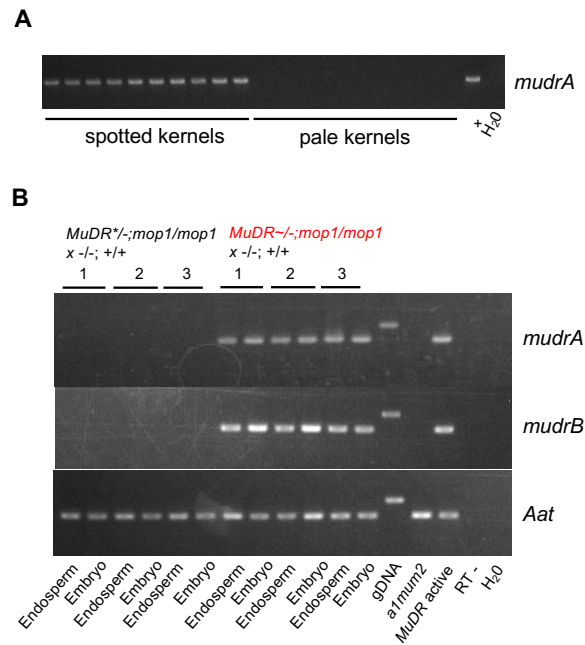
Fig S3. Real-time PCR analysis of *Hsp90* expression in the indicated tissues. Quantitative real-time PCR was performed to measure transcript levels of *ZmHsp90*. Data are the average of two technical replicates collected from ten independent lines. Error bars indicate mean \pm standard deviation (SD) of the ten biological replicates.

933
934
935
936
937
938
939
940
941
942
943



944 **Fig S4. DNA methylation patterns at TIRB of heat-treated H1 *mop1mop1* plants.** DNA
945 methylation patterns at TIRA and TIRB. Ten individual clones were sequenced from each
946 amplification of bisulfite-treated samples with the indicated genotypes. The cytosines in different
947 sequence contexts are represented by different colors (red, CG; blue, CHG; green, CHH, where
948 H=A, C, or T). For each sample, six independent samples were pooled together.

949
950
951
952
953
954
955
956
957
958
959
960



961 **Fig S5. Analysis of *mudrA* and *mudrB* expression in progenies of H1 heat stressed plants.**
962 (A) Genotyping results of an ear from the H2 generation. (B) RT-PCR analysis of *mudrA* and
963 *mudrB* expression in embryos and endosperms from kernels derived from three independent ears

964 derived from crosses of H1 heat stressed plants and control siblings *Aat* is a housekeeping gene
965 that serves as a positive control.

966

967 **References**

968

- 969 1. Arkhipova IR. Neutral Theory, Transposable Elements, and Eukaryotic Genome
970 Evolution. *Mol Biol Evol.* 2018;35(6):1332-7. Epub 2018/04/25. doi: 10.1093/molbev/msy083.
971 PubMed PMID: 29688526; PubMed Central PMCID: PMC6455905.
- 972 2. Hosaka A, Kakutani T. Transposable elements, genome evolution and transgenerational
973 epigenetic variation. *Curr Opin Genet Dev.* 2018;49:43-8. Epub 2018/03/12. doi:
974 10.1016/j.gde.2018.02.012. PubMed PMID: 29525544.
- 975 3. Underwood CJ, Henderson IR, Martienssen RA. Genetic and epigenetic variation of
976 transposable elements in Arabidopsis. *Curr Opin Plant Biol.* 2017;36:135-41. Epub 2017/03/28.
977 doi: 10.1016/j.pbi.2017.03.002. PubMed PMID: 28343122; PubMed Central PMCID:
978 PMC645746046.
- 979 4. Slotkin RK, Freeling M, Lisch D. Heritable transposon silencing initiated by a naturally
980 occurring transposon inverted duplication. *Nat Genet.* 2005;37(6):641-4. Epub 2005/05/24. doi:
981 10.1038/ng1576. PubMed PMID: 15908951.
- 982 5. Bennetzen JL, Wang H. The contributions of transposable elements to the structure,
983 function, and evolution of plant genomes. *Annu Rev Plant Biol.* 2014;65:505-30. Epub
984 2014/03/04. doi: 10.1146/annurev-arplant-050213-035811. PubMed PMID: 24579996.
- 985 6. Lisch D. Epigenetic regulation of transposable elements in plants. *Annu Rev Plant Biol.*
986 2009;60:43-66. Epub 2008/11/15. doi: 10.1146/annurev.arplant.59.032607.092744. PubMed
987 PMID: 19007329.
- 988 7. Grandbastien MA. LTR retrotransposons, handy hitchhikers of plant regulation and stress
989 response. *Biochim Biophys Acta.* 2015;1849(4):403-16. Epub 2014/08/03. doi:
990 10.1016/j.bbagr.2014.07.017. PubMed PMID: 25086340.
- 991 8. Grandbastien MA, Audeon C, Bonnivard E, Casacuberta JM, Chalhoub B, Costa AP, et
992 al. Stress activation and genomic impact of Tnt1 retrotransposons in Solanaceae. *Cytogenet*
993 *Genome Res.* 2005;110(1-4):229-41. Epub 2005/08/12. doi: 10.1159/000084957. PubMed
994 PMID: 16093677.
- 995 9. Ito H, Gaubert H, Bucher E, Mirouze M, Vaillant I, Paszkowski J. An siRNA pathway
996 prevents transgenerational retrotransposition in plants subjected to stress. *Nature.*
997 2011;472(7341):115-9. Epub 2011/03/15. doi: 10.1038/nature09861. PubMed PMID: 21399627.
- 998 10. Kim MY, Zilberman D. DNA methylation as a system of plant genomic immunity.
999 *Trends Plant Sci.* 2014;19(5):320-6. Epub 2014/03/13. doi: 10.1016/j.tplants.2014.01.014.
1000 PubMed PMID: 24618094.
- 1001 11. Zhang H, Lang Z, Zhu JK. Dynamics and function of DNA methylation in plants. *Nat*
1002 *Rev Mol Cell Biol.* 2018;19(8):489-506. Epub 2018/05/23. doi: 10.1038/s41580-018-0016-z.
1003 PubMed PMID: 29784956.
- 1004 12. Law JA, Jacobsen SE. Establishing, maintaining and modifying DNA methylation
1005 patterns in plants and animals. *Nat Rev Genet.* 2010;11(3):204-20. Epub 2010/02/10. doi:
1006 10.1038/nrg2719. PubMed PMID: 20142834; PubMed Central PMCID: PMC3034103.

- 1007 13. Martinez G, Slotkin RK. Developmental relaxation of transposable element silencing in
1008 plants: functional or byproduct? *Curr Opin Plant Biol.* 2012;15(5):496-502. Epub 2012/10/02.
1009 doi: 10.1016/j.pbi.2012.09.001. PubMed PMID: 23022393.
- 1010 14. Noshay JM, Anderson SN, Zhou P, Ji L, Ricci W, Lu Z, et al. Monitoring the interplay
1011 between transposable element families and DNA methylation in maize. *PLoS Genet.*
1012 2019;15(9):e1008291. Epub 2019/09/10. doi: 10.1371/journal.pgen.1008291. PubMed PMID:
1013 31498837; PubMed Central PMCID: PMC6752859.
- 1014 15. Springer NM, Lisch D, Li Q. Creating Order from Chaos: Epigenome Dynamics in Plants
1015 with Complex Genomes. *Plant Cell.* 2016;28(2):314-25. Epub 2016/02/13. doi:
1016 10.1105/tpc.15.00911. PubMed PMID: 26869701; PubMed Central PMCID: PMC6790878.
- 1017 16. Shook MS, Richards EJ. VIM proteins regulate transcription exclusively through the
1018 MET1 cytosine methylation pathway. *Epigenetics.* 2014;9(7):980-6. Epub 2014/04/26. doi:
1019 10.4161/epi.28906. PubMed PMID: 24762702; PubMed Central PMCID: PMC4143413.
- 1020 17. Woo HR, Dittmer TA, Richards EJ. Three SRA-domain methylcytosine-binding proteins
1021 cooperate to maintain global CpG methylation and epigenetic silencing in Arabidopsis. *PLoS*
1022 *Genet.* 2008;4(8):e1000156. Epub 2008/08/16. doi: 10.1371/journal.pgen.1000156. PubMed
1023 PMID: 18704160; PubMed Central PMCID: PMC2491724.
- 1024 18. Chan SW, Henderson IR, Jacobsen SE. Gardening the genome: DNA methylation in
1025 Arabidopsis thaliana. *Nat Rev Genet.* 2005;6(5):351-60. Epub 2005/04/30. doi:
1026 10.1038/nrg1601. PubMed PMID: 15861207.
- 1027 19. Ronemus MJ, Galbiati M, Ticknor C, Chen J, Dellaporta SL. Demethylation-induced
1028 developmental pleiotropy in Arabidopsis. *Science.* 1996;273(5275):654-7. Epub 1996/08/02. doi:
1029 10.1126/science.273.5275.654. PubMed PMID: 8662558.
- 1030 20. Kankel MW, Ramsey DE, Stokes TL, Flowers SK, Haag JR, Jeddloh JA, et al.
1031 Arabidopsis MET1 cytosine methyltransferase mutants. *Genetics.* 2003;163(3):1109-22. Epub
1032 2003/03/29. PubMed PMID: 12663548; PubMed Central PMCID: PMC1462485.
- 1033 21. Du J, Johnson LM, Jacobsen SE, Patel DJ. DNA methylation pathways and their
1034 crosstalk with histone methylation. *Nat Rev Mol Cell Biol.* 2015;16(9):519-32. Epub
1035 2015/08/22. doi: 10.1038/nrm4043. PubMed PMID: 26296162; PubMed Central PMCID:
1036 PMC672940.
- 1037 22. Johnson LM, Bostick M, Zhang X, Kraft E, Henderson I, Callis J, et al. The SRA methyl-
1038 cytosine-binding domain links DNA and histone methylation. *Curr Biol.* 2007;17(4):379-84.
1039 Epub 2007/01/24. doi: 10.1016/j.cub.2007.01.009. PubMed PMID: 17239600; PubMed Central
1040 PMCID: PMC1850948.
- 1041 23. Soppe WJ, Jasencakova Z, Houben A, Kakutani T, Meister A, Huang MS, et al. DNA
1042 methylation controls histone H3 lysine 9 methylation and heterochromatin assembly in
1043 Arabidopsis. *EMBO J.* 2002;21(23):6549-59. Epub 2002/11/29. doi: 10.1093/emboj/cdf657.
1044 PubMed PMID: 12456661; PubMed Central PMCID: PMC136960.
- 1045 24. Wendte JM, Pikaard CS. The RNAs of RNA-directed DNA methylation. *Biochim*
1046 *Biophys Acta Gene Regul Mech.* 2017;1860(1):140-8. Epub 2016/08/16. doi:
1047 10.1016/j.bbagr.2016.08.004. PubMed PMID: 27521981; PubMed Central PMCID:
1048 PMC65203809.
- 1049 25. Matzke M, Kanno T, Daxinger L, Huettel B, Matzke AJ. RNA-mediated chromatin-based
1050 silencing in plants. *Curr Opin Cell Biol.* 2009;21(3):367-76. Epub 2009/02/27. doi:
1051 10.1016/j.ceb.2009.01.025. PubMed PMID: 19243928.

- 1052 26. Matzke MA, Mosher RA. RNA-directed DNA methylation: an epigenetic pathway of
1053 increasing complexity. *Nat Rev Genet.* 2014;15(6):394-408. Epub 2014/05/09. doi:
1054 10.1038/nrg3683. PubMed PMID: 24805120.
- 1055 27. Johnson LM, Du J, Hale CJ, Bischof S, Feng S, Chodavarapu RK, et al. SRA- and SET-
1056 domain-containing proteins link RNA polymerase V occupancy to DNA methylation. *Nature.*
1057 2014;507(7490):124-8. Epub 2014/01/28. doi: 10.1038/nature12931. PubMed PMID: 24463519;
1058 PubMed Central PMCID: PMCPMC3963826.
- 1059 28. Liu W, Duttke SH, Hetzel J, Groth M, Feng S, Gallego-Bartolome J, et al. RNA-directed
1060 DNA methylation involves co-transcriptional small-RNA-guided slicing of polymerase V
1061 transcripts in Arabidopsis. *Nat Plants.* 2018;4(3):181-8. Epub 2018/01/31. doi: 10.1038/s41477-
1062 017-0100-y. PubMed PMID: 29379150; PubMed Central PMCID: PMCPMC5832601.
- 1063 29. Cao X, Aufsatz W, Zilberman D, Mette MF, Huang MS, Matzke M, et al. Role of the
1064 DRM and CMT3 methyltransferases in RNA-directed DNA methylation. *Curr Biol.*
1065 2003;13(24):2212-7. Epub 2003/12/19. doi: 10.1016/j.cub.2003.11.052. PubMed PMID:
1066 14680640.
- 1067 30. Stroud H, Do T, Du J, Zhong X, Feng S, Johnson L, et al. Non-CG methylation patterns
1068 shape the epigenetic landscape in Arabidopsis. *Nat Struct Mol Biol.* 2014;21(1):64-72. Epub
1069 2013/12/18. doi: 10.1038/nsmb.2735. PubMed PMID: 24336224; PubMed Central PMCID:
1070 PMCPMC4103798.
- 1071 31. Zemach A, Kim MY, Hsieh PH, Coleman-Derr D, Eshed-Williams L, Thao K, et al. The
1072 Arabidopsis nucleosome remodeler DDM1 allows DNA methyltransferases to access H1-
1073 containing heterochromatin. *Cell.* 2013;153(1):193-205. Epub 2013/04/02. doi:
1074 10.1016/j.cell.2013.02.033. PubMed PMID: 23540698; PubMed Central PMCID:
1075 PMCPMC4035305.
- 1076 32. Wendte JM, Schmitz RJ. Specifications of Targeting Heterochromatin Modifications in
1077 Plants. *Mol Plant.* 2018;11(3):381-7. Epub 2017/10/17. doi: 10.1016/j.molp.2017.10.002.
1078 PubMed PMID: 29032247.
- 1079 33. Li Q, Gent JI, Zynda G, Song J, Makarevitch I, Hirsch CD, et al. RNA-directed DNA
1080 methylation enforces boundaries between heterochromatin and euchromatin in the maize
1081 genome. *Proc Natl Acad Sci U S A.* 2015;112(47):14728-33. Epub 2015/11/11. doi:
1082 10.1073/pnas.1514680112. PubMed PMID: 26553984; PubMed Central PMCID:
1083 PMCPMC4664327.
- 1084 34. Alleman M, Sidorenko L, McGinnis K, Seshadri V, Dorweiler JE, White J, et al. An
1085 RNA-dependent RNA polymerase is required for paramutation in maize. *Nature.*
1086 2006;442(7100):295-8. Epub 2006/07/21. doi: 10.1038/nature04884. PubMed PMID: 16855589.
- 1087 35. Woodhouse MR, Freeling M, Lisch D. The mop1 (mediator of paramutation1) mutant
1088 progressively reactivates one of the two genes encoded by the MuDR transposon in maize.
1089 *Genetics.* 2006;172(1):579-92. Epub 2005/10/13. doi: 10.1534/genetics.105.051383. PubMed
1090 PMID: 16219782; PubMed Central PMCID: PMCPMC1456185.
- 1091 36. Nobuta K, Lu C, Shrivastava R, Pillay M, De Paoli E, Accerbi M, et al. Distinct size
1092 distribution of endogenous siRNAs in maize: Evidence from deep sequencing in the mop1-1
1093 mutant. *Proc Natl Acad Sci U S A.* 2008;105(39):14958-63. Epub 2008/09/26. doi:
1094 10.1073/pnas.0808066105. PubMed PMID: 18815367; PubMed Central PMCID:
1095 PMCPMC2567475.
- 1096 37. Jia Y, Lisch DR, Ohtsu K, Scanlon MJ, Nettleton D, Schnable PS. Loss of RNA-
1097 dependent RNA polymerase 2 (RDR2) function causes widespread and unexpected changes in

- 1098 the expression of transposons, genes, and 24-nt small RNAs. *PLoS Genet.* 2009;5(11):e1000737.
1099 Epub 2009/11/26. doi: 10.1371/journal.pgen.1000737. PubMed PMID: 19936292; PubMed
1100 Central PMCID: PMCPMC2774947.
- 1101 38. Heard E, Martienssen RA. Transgenerational epigenetic inheritance: myths and
1102 mechanisms. *Cell.* 2014;157(1):95-109. Epub 2014/04/01. doi: 10.1016/j.cell.2014.02.045.
1103 PubMed PMID: 24679529; PubMed Central PMCID: PMCPMC4020004.
- 1104 39. Tsukahara S, Kobayashi A, Kawabe A, Mathieu O, Miura A, Kakutani T. Bursts of
1105 retrotransposition reproduced in *Arabidopsis*. *Nature.* 2009;461(7262):423-6. Epub 2009/09/08.
1106 doi: 10.1038/nature08351. PubMed PMID: 19734880.
- 1107 40. Lippman Z, May B, Yordan, Singer T, Martienssen R. Distinct Mechanisms Determine
1108 Transposon Inheritance and Methylation via Small Interfering RNA and Histone Modification.
1109 *PLoS Biol.* 2003;1(3):420. doi: 10.1371/journal.pbio.0000067
1110 10.1371/journal.pbio.0000067.g001.
- 1111 41. Teixeira FK, Heredia F, Sarazin A, Roudier F, Boccara M, Ciaudo C, et al. A role for
1112 RNAi in the selective correction of DNA methylation defects. *Science.* 2009;323(5921):1600-4.
1113 Epub 2009/01/31. doi: 10.1126/science.1165313. PubMed PMID: 19179494.
- 1114 42. To TK, Nishizawa Y, Inagaki S, Tarutani Y, Tominaga S, Toyoda A, et al. RNA
1115 interference-independent reprogramming of DNA methylation in *Arabidopsis*. *Nat Plants.* 2020.
1116 Epub 2020/12/02. doi: 10.1038/s41477-020-00810-z. PubMed PMID: 33257860.
- 1117 43. Schuettengruber B, Bourbon HM, Di Croce L, Cavalli G. Genome Regulation by
1118 Polycomb and Trithorax: 70 Years and Counting. *Cell.* 2017;171(1):34-57. Epub 2017/09/25.
1119 doi: 10.1016/j.cell.2017.08.002. PubMed PMID: 28938122.
- 1120 44. Mozgova I, Hennig L. The polycomb group protein regulatory network. *Annu Rev Plant*
1121 *Biol.* 2015;66:269-96. Epub 2015/01/27. doi: 10.1146/annurev-arplant-043014-115627. PubMed
1122 PMID: 25621513.
- 1123 45. Steffen PA, Ringrose L. What are memories made of? How Polycomb and Trithorax
1124 proteins mediate epigenetic memory. *Nat Rev Mol Cell Biol.* 2014;15(5):340-56. Epub
1125 2014/04/24. doi: 10.1038/nrm3789. PubMed PMID: 24755934.
- 1126 46. Xiao J, Wagner D. Polycomb repression in the regulation of growth and development in
1127 *Arabidopsis*. *Curr Opin Plant Biol.* 2015;23:15-24. Epub 2014/12/03. doi:
1128 10.1016/j.pbi.2014.10.003. PubMed PMID: 25449722.
- 1129 47. Roudier F, Ahmed I, Berard C, Sarazin A, Mary-Huard T, Cortijo S, et al. Integrative
1130 epigenomic mapping defines four main chromatin states in *Arabidopsis*. *EMBO J.*
1131 2011;30(10):1928-38. Epub 2011/04/14. doi: 10.1038/emboj.2011.103. PubMed PMID:
1132 21487388; PubMed Central PMCID: PMCPMC3098477.
- 1133 48. Costa S, Dean C. Storing memories: the distinct phases of Polycomb-mediated silencing
1134 of *Arabidopsis* FLC. *Biochem Soc Trans.* 2019;47(4):1187-96. Epub 2019/07/07. doi:
1135 10.1042/BST20190255. PubMed PMID: 31278155.
- 1136 49. Searle I, He Y, Turck F, Vincent C, Fornara F, Krober S, et al. The transcription factor
1137 FLC confers a flowering response to vernalization by repressing meristem competence and
1138 systemic signaling in *Arabidopsis*. *Genes Dev.* 2006;20(7):898-912. Epub 2006/04/08. doi:
1139 10.1101/gad.373506. PubMed PMID: 16600915; PubMed Central PMCID: PMCPMC1472290.
- 1140 50. Crevillen P, Yang H, Cui X, Greeff C, Trick M, Qiu Q, et al. Epigenetic reprogramming
1141 that prevents transgenerational inheritance of the vernalized state. *Nature.* 2014;515(7528):587-
1142 90. Epub 2014/09/16. doi: 10.1038/nature13722. PubMed PMID: 25219852; PubMed Central
1143 PMCID: PMCPMC4247276.

- 1144 51. Tao Z, Shen L, Gu X, Wang Y, Yu H, He Y. Embryonic epigenetic reprogramming by a
1145 pioneer transcription factor in plants. *Nature*. 2017;551(7678):124-8. Epub 2017/10/27. doi:
1146 10.1038/nature24300. PubMed PMID: 29072296.
- 1147 52. Borg M, Jacob Y, Susaki D, LeBlanc C, Buendia D, Axelsson E, et al. Targeted
1148 reprogramming of H3K27me3 resets epigenetic memory in plant paternal chromatin. *Nat Cell*
1149 *Biol*. 2020;22(6):621-9. Epub 2020/05/13. doi: 10.1038/s41556-020-0515-y. PubMed PMID:
1150 32393884.
- 1151 53. Michael TP. Plant genome size variation: bloating and purging DNA. *Brief Funct*
1152 *Genomics*. 2014;13(4):308-17. Epub 2014/03/22. doi: 10.1093/bfgp/elu005. PubMed PMID:
1153 24651721.
- 1154 54. Naito K, Zhang F, Tsukiyama T, Saito H, Hancock CN, Richardson AO, et al.
1155 Unexpected consequences of a sudden and massive transposon amplification on rice gene
1156 expression. *Nature*. 2009;461(7267):1130-4. Epub 2009/10/23. doi: 10.1038/nature08479.
1157 PubMed PMID: 19847266.
- 1158 55. Wessler SR. Turned on by stress. *Plant retrotransposons*. *Curr Biol*. 1996;6(8):959-61.
1159 Epub 1996/08/01. doi: 10.1016/s0960-9822(02)00638-3. PubMed PMID: 8805314.
- 1160 56. Woodrow P, Pontecorvo G, Ciarmiello LF, Fuggi A, Carillo P. Ttd1a promoter is
1161 involved in DNA-protein binding by salt and light stresses. *Mol Biol Rep*. 2011;38(6):3787-94.
1162 Epub 2010/11/26. doi: 10.1007/s11033-010-0494-3. PubMed PMID: 21104438.
- 1163 57. Kimura Y, Tosa Y, Shimada S, Sogo R, Kusaba M, Sunaga T, et al. OARE-1, a Ty1-
1164 copia retrotransposon in oat activated by abiotic and biotic stresses. *Plant Cell Physiol*.
1165 2001;42(12):1345-54. Epub 2002/01/05. doi: 10.1093/pcp/pce171. PubMed PMID: 11773527.
- 1166 58. Makarevitch I, Waters AJ, West PT, Stitzer M, Hirsch CN, Ross-Ibarra J, et al.
1167 Transposable elements contribute to activation of maize genes in response to abiotic stress. *PLoS*
1168 *Genet*. 2015;11(1):e1004915. Epub 2015/01/09. doi: 10.1371/journal.pgen.1004915. PubMed
1169 PMID: 25569788; PubMed Central PMCID: PMC4287451.
- 1170 59. Kashkush K, Feldman M, Levy AA. Transcriptional activation of retrotransposons alters
1171 the expression of adjacent genes in wheat. *Nat Genet*. 2003;33(1):102-6. Epub 2002/12/17. doi:
1172 10.1038/ng1063. PubMed PMID: 12483211.
- 1173 60. Lang-Mladek C, Popova O, Kiok K, Berlinger M, Rakic B, Aufsatz W, et al.
1174 Transgenerational inheritance and resetting of stress-induced loss of epigenetic gene silencing in
1175 *Arabidopsis*. *Mol Plant*. 2010;3(3):594-602. Epub 2010/04/23. doi: 10.1093/mp/ssq014. PubMed
1176 PMID: 20410255; PubMed Central PMCID: PMC4287484.
- 1177 61. Molinier J, Ries G, Zipfel C, Hohn B. Transgeneration memory of stress in plants.
1178 *Nature*. 2006;442(7106):1046-9. Epub 2006/08/08. doi: 10.1038/nature05022. PubMed PMID:
1179 16892047.
- 1180 62. Cavrak VV, Lettner N, Jamge S, Kosarewicz A, Bayer LM, Mittelsten Scheid O. How a
1181 retrotransposon exploits the plant's heat stress response for its activation. *PLoS Genet*.
1182 2014;10(1):e1004115. Epub 2014/02/06. doi: 10.1371/journal.pgen.1004115. PubMed PMID:
1183 24497839; PubMed Central PMCID: PMC4287484.
- 1184 63. Ohtsu K, Smith MB, Emrich SJ, Borsuk LA, Zhou R, Chen T, et al. Global gene
1185 expression analysis of the shoot apical meristem of maize (*Zea mays* L.). *Plant J*.
1186 2007;52(3):391-404. Epub 2007/09/04. doi: 10.1111/j.1365-3113.2007.03244.x. PubMed
1187 PMID: 17764504; PubMed Central PMCID: PMC4287484.
- 1188 64. Baubec T, Finke A, Mittelsten Scheid O, Pecinka A. Meristem-specific expression of
1189 epigenetic regulators safeguards transposon silencing in *Arabidopsis*. *EMBO Rep*.

- 1190 2014;15(4):446-52. Epub 2014/02/25. doi: 10.1002/embr.201337915. PubMed PMID:
1191 24562611; PubMed Central PMCID: PMC3989676.
- 1192 65. Iwasaki M, Paszkowski J. Identification of genes preventing transgenerational
1193 transmission of stress-induced epigenetic states. *Proc Natl Acad Sci U S A*. 2014;111(23):8547-
1194 52. Epub 2014/06/10. doi: 10.1073/pnas.1402275111. PubMed PMID: 24912148; PubMed
1195 Central PMCID: PMC4060648.
- 1196 66. Mathieu O, Reinders J, Caikovski M, Smathajitt C, Paszkowski J. Transgenerational
1197 stability of the Arabidopsis epigenome is coordinated by CG methylation. *Cell*.
1198 2007;130(5):851-62. Epub 2007/09/07. doi: 10.1016/j.cell.2007.07.007. PubMed PMID:
1199 17803908.
- 1200 67. Lippman Z, May B, Yordan C, Singer T, Martienssen R. Distinct mechanisms determine
1201 transposon inheritance and methylation via small interfering RNA and histone modification.
1202 *PLoS Biol*. 2003;1(3):E67. Epub 2003/12/24. doi: 10.1371/journal.pbio.0000067. PubMed
1203 PMID: 14691539; PubMed Central PMCID: PMC300680.
- 1204 68. Sigman MJ, Slotkin RK. The First Rule of Plant Transposable Element Silencing:
1205 Location, Location, Location. *Plant Cell*. 2016;28(2):304-13. Epub 2016/02/13. doi:
1206 10.1105/tpc.15.00869. PubMed PMID: 26869697; PubMed Central PMCID: PMC4790875.
- 1207 69. Lisch D. Mutator and MULE Transposons. *Microbiol Spectr*. 2015;3(2):MDNA3-0032-
1208 2014. Epub 2015/06/25. doi: 10.1128/microbiolspec.MDNA3-0032-2014. PubMed PMID:
1209 26104710.
- 1210 70. Lisch D. Mutator transposons. *Trends Plant Sci*. 2002;7(11):498-504. Epub 2002/11/06.
1211 doi: 10.1016/s1360-1385(02)02347-6. PubMed PMID: 12417150.
- 1212 71. Lisch D, Girard L, Donlin M, Freeling M. Functional analysis of deletion derivatives of
1213 the maize transposon MuDR delineates roles for the MURA and MURB proteins. *Genetics*.
1214 1999;151(1):331-41. Epub 1999/01/05. PubMed PMID: 9872971; PubMed Central PMCID:
1215 PMC1460458.
- 1216 72. Rudenko GN, Walbot V. Expression and post-transcriptional regulation of maize
1217 transposable element MuDR and its derivatives. *Plant Cell*. 2001;13(3):553-70. Epub
1218 2001/03/17. doi: 10.1105/tpc.13.3.553. PubMed PMID: 11251096; PubMed Central PMCID:
1219 PMC135511.
- 1220 73. Slotkin RK, Freeling M, Lisch D. Mu killer causes the heritable inactivation of the
1221 Mutator family of transposable elements in *Zea mays*. *Genetics*. 2003;165(2):781-97. Epub
1222 2003/10/24. PubMed PMID: 14573488; PubMed Central PMCID: PMC1462800.
- 1223 74. Lisch D, Chomet P, Freeling M. Genetic characterization of the Mutator system in maize:
1224 behavior and regulation of Mu transposons in a minimal line. *Genetics*. 1995;139(4):1777-96.
1225 Epub 1995/04/01. PubMed PMID: 7789777; PubMed Central PMCID: PMC1206502.
- 1226 75. Li H, Freeling M, Lisch D. Epigenetic reprogramming during vegetative phase change in
1227 maize. *Proc Natl Acad Sci U S A*. 2010;107(51):22184-9. Epub 2010/12/08. doi:
1228 10.1073/pnas.1016884108. PubMed PMID: 21135217; PubMed Central PMCID:
1229 PMC3009802.
- 1230 76. Burgess D, Li H, Zhao M, Kim SY, Lisch D. Silencing of Mutator Elements in Maize
1231 Involves Distinct Populations of Small RNAs and Distinct Patterns of DNA Methylation.
1232 *Genetics*. 2020;215(2):379-91. Epub 2020/04/02. doi: 10.1534/genetics.120.303033. PubMed
1233 PMID: 32229532; PubMed Central PMCID: PMC7268996.
- 1234 77. Lisch D, Carey CC, Dorweiler JE, Chandler VL. A mutation that prevents paramutation
1235 in maize also reverses Mutator transposon methylation and silencing. *Proc Natl Acad Sci U S A*.

- 1236 2002;99(9):6130-5. Epub 2002/04/18. doi: 10.1073/pnas.052152199. PubMed PMID: 11959901;
1237 PubMed Central PMCID: PMCPMC122914.
- 1238 78. Woodhouse MR, Freeling M, Lisch D. Initiation, establishment, and maintenance of
1239 heritable MuDR transposon silencing in maize are mediated by distinct factors. *PLoS Biol.*
1240 2006;4(10):e339. Epub 2006/09/14. doi: 10.1371/journal.pbio.0040339. PubMed PMID:
1241 16968137; PubMed Central PMCID: PMCPMC1563492.
- 1242 79. Kenchanmane Raju SK, Ritter EJ, Niederhuth CE. Establishment, maintenance, and
1243 biological roles of non-CG methylation in plants. *Essays Biochem.* 2019;63(6):743-55. Epub
1244 2019/10/28. doi: 10.1042/EBC20190032. PubMed PMID: 31652316; PubMed Central PMCID:
1245 PMCPMC6923318.
- 1246 80. Poethig RS. The Maize Shoot. In: Freeling M. WV, editor. *The Maize Handbook* New
1247 York, NY.: Springer; 1994. p. 11-7.
- 1248 81. Hanway J. *How a Corn Plant Develops*. Des Moines, IA: Iowa State University, 1966.
- 1249 82. Du J, Johnson LM, Groth M, Feng S, Hale CJ, Li S, et al. Mechanism of DNA
1250 methylation-directed histone methylation by KRYPTONITE. *Mol Cell.* 2014;55(3):495-504.
1251 Epub 2014/07/16. doi: 10.1016/j.molcel.2014.06.009. PubMed PMID: 25018018; PubMed
1252 Central PMCID: PMCPMC4127122.
- 1253 83. Amedeo P, Habu Y, Afsar K, Mittelsten Scheid O, Paszkowski J. Disruption of the plant
1254 gene MOM releases transcriptional silencing of methylated genes. *Nature.* 2000;405(6783):203-
1255 6. Epub 2000/05/23. doi: 10.1038/35012108. PubMed PMID: 10821279.
- 1256 84. Caikovski M, Yokthongwattana C, Habu Y, Nishimura T, Mathieu O, Paszkowski J.
1257 Divergent evolution of CHD3 proteins resulted in MOM1 refining epigenetic control in vascular
1258 plants. *PLoS Genet.* 2008;4(8):e1000165. Epub 2008/08/30. doi: 10.1371/journal.pgen.1000165.
1259 PubMed PMID: 18725928; PubMed Central PMCID: PMCPMC2507757.
- 1260 85. Probst AV, Fransz PF, Paszkowski J, Mittelsten Scheid O. Two means of transcriptional
1261 reactivation within heterochromatin. *Plant J.* 2003;33(4):743-9. Epub 2003/03/01. doi:
1262 10.1046/j.1365-313x.2003.01667.x. PubMed PMID: 12609046.
- 1263 86. Moissiard G, Cokus SJ, Cary J, Feng S, Billi AC, Stroud H, et al. MORC family ATPases
1264 required for heterochromatin condensation and gene silencing. *Science.* 2012;336(6087):1448-
1265 51. Epub 2012/05/05. doi: 10.1126/science.1221472. PubMed PMID: 22555433; PubMed
1266 Central PMCID: PMCPMC3376212.
- 1267 87. Jacob Y, Feng S, LeBlanc CA, Bernatavichute YV, Stroud H, Cokus S, et al. ATXR5 and
1268 ATXR6 are H3K27 monomethyltransferases required for chromatin structure and gene silencing.
1269 *Nat Struct Mol Biol.* 2009;16(7):763-8. Epub 2009/06/09. doi: 10.1038/nsmb.1611. PubMed
1270 PMID: 19503079; PubMed Central PMCID: PMCPMC2754316.
- 1271 88. Harris CJ, Husmann D, Liu W, Kasmi FE, Wang H, Papikian A, et al. Arabidopsis
1272 AtMORC4 and AtMORC7 Form Nuclear Bodies and Repress a Large Number of Protein-
1273 Coding Genes. *PLoS Genet.* 2016;12(5):e1005998. Epub 2016/05/14. doi:
1274 10.1371/journal.pgen.1005998. PubMed PMID: 27171361; PubMed Central PMCID:
1275 PMCPMC4865129.
- 1276 89. Ikeda Y, Pelissier T, Bourguet P, Becker C, Pouch-Pelissier MN, Pogorelnik R, et al.
1277 Arabidopsis proteins with a transposon-related domain act in gene silencing. *Nat Commun.*
1278 2017;8:15122. Epub 2017/05/04. doi: 10.1038/ncomms15122. PubMed PMID: 28466841;
1279 PubMed Central PMCID: PMCPMC5418596.

- 1280 90. Hayashi Y, Takehira K, Nozawa K, Suzuki T, Masuta Y, Kato A, et al. ONSEN shows
1281 different transposition activities in RdDM pathway mutants. *Genes Genet Syst.* 2020. Epub
1282 2020/09/08. doi: 10.1266/ggs.20-00019. PubMed PMID: 32893196.
- 1283 91. Matsunaga W, Kobayashi A, Kato A, Ito H. The effects of heat induction and the siRNA
1284 biogenesis pathway on the transgenerational transposition of ONSEN, a copia-like
1285 retrotransposon in *Arabidopsis thaliana*. *Plant Cell Physiol.* 2012;53(5):824-33. Epub
1286 2011/12/17. doi: 10.1093/pcp/pcr179. PubMed PMID: 22173101.
- 1287 92. Chomet P, Lisch D, Hardeman KJ, Chandler VL, Freeling M. Identification of a
1288 regulatory transposon that controls the Mutator transposable element system in maize. *Genetics.*
1289 1991;129(1):261-70. Epub 1991/09/01. PubMed PMID: 1657702; PubMed Central PMCID:
1290 PMCPMC1204575.
- 1291 93. Kato M, Takashima K, Kakutani T. Epigenetic control of CACTA transposon mobility in
1292 *Arabidopsis thaliana*. *Genetics.* 2004;168(2):961-9. Epub 2004/10/30. doi:
1293 10.1534/genetics.104.029637. PubMed PMID: 15514067; PubMed Central PMCID:
1294 PMCPMC1448851.
- 1295 94. Mari-Ordonez A, Marchais A, Etcheverry M, Martin A, Colot V, Voinnet O.
1296 Reconstructing de novo silencing of an active plant retrotransposon. *Nat Genet.*
1297 2013;45(9):1029-39. Epub 2013/07/16. doi: 10.1038/ng.2703. PubMed PMID: 23852169.
- 1298 95. Hirochika H, Sugimoto K, Otsuki Y, Tsugawa H, Kanda M. Retrotransposons of rice
1299 involved in mutations induced by tissue culture. *Proc Natl Acad Sci U S A.* 1996;93(15):7783-8.
1300 Epub 1996/07/23. doi: 10.1073/pnas.93.15.7783. PubMed PMID: 8755553; PubMed Central
1301 PMCID: PMCPMC38825.
- 1302 96. Sheldon CC, Hills MJ, Lister C, Dean C, Dennis ES, Peacock WJ. Resetting of
1303 FLOWERING LOCUS C expression after epigenetic repression by vernalization. *Proc Natl*
1304 *Acad Sci U S A.* 2008;105(6):2214-9. Epub 2008/02/06. doi: 10.1073/pnas.0711453105.
1305 PubMed PMID: 18250331; PubMed Central PMCID: PMCPMC2542874.
- 1306 97. Li C, Gu L, Gao L, Chen C, Wei CQ, Qiu Q, et al. Concerted genomic targeting of
1307 H3K27 demethylase REF6 and chromatin-remodeling ATPase BRM in *Arabidopsis*. *Nat Genet.*
1308 2016;48(6):687-93. Epub 2016/04/26. doi: 10.1038/ng.3555. PubMed PMID: 27111034;
1309 PubMed Central PMCID: PMCPMC5134324.
- 1310 98. Liu J, Feng L, Gu X, Deng X, Qiu Q, Li Q, et al. An H3K27me3 demethylase-HSFA2
1311 regulatory loop orchestrates transgenerational thermomemory in *Arabidopsis*. *Cell Res.*
1312 2019;29(5):379-90. Epub 2019/02/20. doi: 10.1038/s41422-019-0145-8. PubMed PMID:
1313 30778176; PubMed Central PMCID: PMCPMC6796840.
- 1314 99. Cui X, Lu F, Qiu Q, Zhou B, Gu L, Zhang S, et al. REF6 recognizes a specific DNA
1315 sequence to demethylate H3K27me3 and regulate organ boundary formation in *Arabidopsis*. *Nat*
1316 *Genet.* 2016;48(6):694-9. Epub 2016/04/26. doi: 10.1038/ng.3556. PubMed PMID: 27111035.
- 1317 100. Montgomery SA, Tanizawa Y, Galik B, Wang N, Ito T, Mochizuki T, et al. Chromatin
1318 Organization in Early Land Plants Reveals an Ancestral Association between H3K27me3,
1319 Transposons, and Constitutive Heterochromatin. *Curr Biol.* 2020;30(4):573-88 e7. Epub
1320 2020/02/01. doi: 10.1016/j.cub.2019.12.015. PubMed PMID: 32004456; PubMed Central
1321 PMCID: PMCPMC7209395.
- 1322 101. Moreno-Romero J, Del Toro-De Leon G, Yadav VK, Santos-Gonzalez J, Kohler C.
1323 Epigenetic signatures associated with imprinted paternally expressed genes in the *Arabidopsis*
1324 endosperm. *Genome Biol.* 2019;20(1):41. Epub 2019/02/23. doi: 10.1186/s13059-019-1652-0.
1325 PubMed PMID: 30791924; PubMed Central PMCID: PMCPMC6385439.

- 1326 102. Frapporti A, Miro Pina C, Arnaiz O, Holoch D, Kawaguchi T, Humbert A, et al. The
1327 Polycomb protein Ezh1 mediates H3K9 and H3K27 methylation to repress transposable elements
1328 in *Paramecium*. *Nat Commun.* 2019;10(1):2710. Epub 2019/06/22. doi: 10.1038/s41467-019-
1329 10648-5. PubMed PMID: 31221974; PubMed Central PMCID: PMC6586856.
- 1330 103. Gruntman E, Qi Y, Slotkin RK, Roeder T, Martienssen RA, Sachidanandam R. Kismeth:
1331 analyzer of plant methylation states through bisulfite sequencing. *BMC Bioinformatics.*
1332 2008;9:371. Epub 2008/09/13. doi: 10.1186/1471-2105-9-371. PubMed PMID: 18786255;
1333 PubMed Central PMCID: PMC653349.
- 1334 104. He L, Wu W, Zinta G, Yang L, Wang D, Liu R, et al. A naturally occurring epiallele
1335 associates with leaf senescence and local climate adaptation in *Arabidopsis* accessions. *Nat*
1336 *Commun.* 2018;9(1):460. Epub 2018/02/02. doi: 10.1038/s41467-018-02839-3. PubMed PMID:
1337 29386641; PubMed Central PMCID: PMC5792623.
- 1338 105. Carter B, Bishop B, Ho KK, Huang R, Jia W, Zhang H, et al. The Chromatin Remodelers
1339 PKL and PIE1 Act in an Epigenetic Pathway That Determines H3K27me3 Homeostasis in
1340 *Arabidopsis*. *Plant Cell.* 2018;30(6):1337-52. Epub 2018/05/29. doi: 10.1105/tpc.17.00867.
1341 PubMed PMID: 29802212; PubMed Central PMCID: PMC6048792.
- 1342 106. Haring M, Offermann S, Danker T, Horst I, Peterhansel C, Stam M. Chromatin
1343 immunoprecipitation: optimization, quantitative analysis and data normalization. *Plant Methods.*
1344 2007;3:11. Epub 2007/09/26. doi: 10.1186/1746-4811-3-11. PubMed PMID: 17892552; PubMed
1345 Central PMCID: PMC2077865.
- 1346